

**Experimental Modelling of the Fluid Flow in a Furnace Top of an Ethane Cracker in
EPEMSB, Paka.**

by

**Mohd Alif Syazwan bin Mohd Nasir
5851
Mechanical Engineering**

**Final Report submitted in partial fulfilment of
the requirements for the
Bachelor of Engineering (Hons)
(Mechanical Engineering)**

JANUARY 2008

**Universiti Teknologi PETRONAS
Bandar Seri Iskandar
31750 Tronoh
Perak Darul Ridzuan**

CERTIFICATION OF APPROVAL

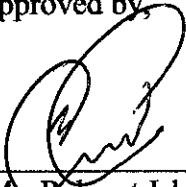
**Experimental Modelling of the Fluid Flow in a Furnace Top of an Ethane Cracker
at EPMSB Paka**

by

Mohd Alif Syazwan bin Mohd Nasir

A project dissertation submitted to the
Mechanical Engineering Programme
Universiti Teknologi PETRONAS
in partial fulfilment of the requirement for the
BACHELOR OF ENGINEERING (Hons)
(MECHANICAL ENGINEERING)

Approved by,



(Mr. Rahmat Iskandar Shazi)

UNIVERSITI TEKNOLOGI PETRONAS

TRONOH, PERAK

January 2008

CERTIFICATION OF ORIGINALITY

This is to certify that I am responsible for the work submitted in this project, that the original work is my own except as specified in the references and acknowledgements, and that the original work contained herein have not been undertaken or done by unspecified sources or persons.



MOHD ALIF SYAZWAN BIN MOHD NASIR

ABSTRACT

The problem encountered is the induction fan of an ethane cracking furnace at Ethylene Polyethylene Malaysia Sdn Bhd (EPEMSB) failed suspected due to induced turbulence. A model of a furnace top must be created to simulate the flow in the furnace top to analyze it, troubleshoot the possible root causes and postulate methods or approaches to prevent reoccurrences. From the previous FYP, this model were experimented but there is several problem encountered during the experiment. One of the problem is there is leaking within the test rig, improper pump selection, bubble air trapped in the top of the test section and the shift of the centre of mass of the damper flapper system. The test rig must be modified to overcome these problems, which is the main subject matter of this documentation. From the previous experiment, the root cause of the problem is the high induced turbulence in the furnace top. However there is a need to analyze the possible root cause of the induced turbulence.

ACKNOWLEDGEMENT

First and foremost I would like to thank God Almighty for being my strength in times of needs and my place of comfort. With God, all things are possible.

With my deepest sense of gratitude, I would like to express my utmost and sincerest thanks to my supervisor, Mr. Rahmat Iskandar Shazi for his guidance, suggestions and feedback for the entire period of this project. Mr. Rahmat provided me with never ending encouragement and support to endure this entire project. I thank Mr. Rahmat for his patience and helpfulness at all times.

I would also like to express my sincere thanks to my family, my friends, UTP technicians and to all person who have given me enormous amounts of supports, motivation and assistance during the entire period of the project.. Each individual showed tremendous support, training and sacrifice of time and energy to help me.

I also gratefully acknowledge the Mechanical Engineering Department of Universiti Teknologi Petronas for providing the sufficient guidance to complete this project smoothly. I also thank the department for the funding of the materials and equipment used for this project.

I will cherish the contributions, support and encouragement of the people above in my heart forever.

TABLE OF CONTENTS

ABSTRACT		i	
CHAPTER 1	INTRODUCTION		1
	1.1	Background	1
	1.2	Problem Statement	3
	1.3	Objectives	3
	1.4	Scope of Study	3
CHAPTER 2			4
LITERATURE REVIEW		4	
2.1	Ethane Cracking Furnace	4	
	2.1.1 Brief Description of The Furnace	4	
	2.1.2 Brief Description of ethane	6	
	2.1.3 Brief Description of the Cracking Process	7	
2.2	Laminar Flow	8	
2.3	Transitional Flow	8	
2.4	Turbulent Flow	8	
2.5	Friction Drag	9	
2.6	Pump Type	10	
2.7	Dimensional Analysis	17	
	2.7.1 Reynolds Number	17	
	2.7.2 Mach Number	18	
	2.7.3 Prandtl Number	18	
	2.7.4 Nusselt Number	19	
2.8	Continuity Equation	19	
	2.8.1 Venturi	20	
2.9	The Ideal Gas	20	
	2.9.1 The Properties of the Ideal Gases	21	
	2.9.2 Dalton's Law	22	
	2.9.3 Amangat's Law	23	
	2.9.4 Apparent Molecular Weight and Specific Gravity of Gases in Mixture	23	
2.10	Flow in Non-Circular Conduit	23	
2.11	Honeycombs And Screens	24	
2.12	Center of Mass	25	
2.13	Torque Sequence	25	
2.14	Manometer	27	
2.15	Flue Gas Stack Draft	32	
Chapter 3			34
METHODOLOGY		34	
3.1	Description of Methodology Used In The Study	34	
3.2	Dimensional Similarity	35	
3.3	Designing the Test Rig	35	
	3.3.1 Engineering drawing	36	

	3.4	Fabrication	40
		3.4.1	Test Rig
		3.4.2	Visualization Kit
		3.4.3	Gasket
		3.4.4	Base of the Test Rig
		3.4.5	Top Cover of the Container
		3.4.6	Piping System
		3.4.7	Tee Support
	3.5	The Pump Requirement	45
	3.6	Material Procurement	46
		3.6.1	Inventory List
	3.7	Methodology of The Experiment	48
CHAPTER 4	RESULTS AND DISCUSSION		51
	4.1	Results	51
		4.1.1	Flow Visualization
	4.2	Discussion	52
		4.2.1	Interpretation of The Results
		4.2.2	Probable Root Causes
		4.2.3	Compressibility of The Fluids
		4.2.4	Limitations
CHAPTER 5	CONCLUSION AND RECOMMENDATIONS		59
	5.1	Conclusion	59
	5.2	Recommendation	63
LIST OF TABLES			ii
LIST OF FIGURES			ii
REFERENCE			iv
APPENDIX I			v
APPENDIX II			x
APPENDIX III			xi

List of Tables.

Table 3.1: Item Purchased/Obtained for Fabrication	47
Table 3.2: Consumable Purchased/Obtained for Fabrication	48

List of Figures.

Figure 1.1: Induction fan	2
Figure 1.2: Cowling	2
Figure 1.3: Cotter pin and linkage close up	2
Figure 1.4: Assembly of cotter pins and linkage	2
Figure 1.5: Broken cotter pin	2
Figure 2.1: Industrial furnaces diagram.	5
Figure 2.2: Laminar and turbulent water flow over the hull of a submarine	9
Figure 2.3: Axial flow pump propeller	10
Figure 2.4: Model AF/MPAF Axial Flow Pump	11
Figure 2.5: Typical axial flow pump performance curve	11
Figure 2.6: A schematic of a typical centrifugal pump	13
Figure 2.7: A typical performance curve of a centrifugal pump	14
Figure 2.8: Model Prime Line® Centrifugal Pump	14
Figure 2.9: Typical performance curve of a centrifugal pump	15
Figure 2.10: Comparison of performance curves of typical centrifugal reciprocating pumps at constant speed	16
Figure 2.11: The three-dimensional geometry of a honeycomb cell	24
Figure 2.12: Centre of mass illustration	25
Figure 2.13: Torque sequences for bolt patterns	26
Figure 2.14: Illustration of a basic manometer design	27
Figure 2.15: U-shaped manometer with both end open to the atmosphere	28
Figure 2.16: U-shaped manometer with one closed end	29
Figure 2.17: U-shaped manometer with one closed end	30
Figure 2.18: A cylinder illustration for deriving the pressure equation	31
Figure 2.19: The stack effect in chimneys: the gauges represent absolute air pressure and the airflow is indicated with light grey arrows. The gauge dials move clockwise with increasing pressure	33
Figure 3.1: Orthographic drawing of Main Compartment	36
Figure 3.2: Orthographic drawing of Diffuser Compartment	37
Figure 3.3: Orthographic Drawing of Damper Flapper Compartment	37
Figure 3.4: Orthographic Drawing of Outlet Nozzle	38
Figure 3.5: Test rig assembly	39
Figure 3.6: Main compartment	40

Figure 3.7: Diffuser compartment	41
Figure 3.8: Damper flapper compartment	41
Figure 3.9: O-ring placement in the Perspex shell	42
Figure 3.10: Outlet nozzle	42
Figure 3.11: Water container	42
Figure 3.12: The visualization Kit	43
Figure 3.13: Gaskets	43
Figure 3.14: Bottom view of the base	44
Figure 3.15: Top view of the base	44
Figure 3.16: Top cover of the container	44
Figure 3.17: Piping system	45
Figure 3.18: Tee support	45
Figure 3.19: Test rig assembly and arrangement	49
Figure 3.20: Manometer panel	50
Figure 4.1: Sample Images of Flow Visualization	52
Figure 4.2: The positions of the damper flapper	53
Figure 4.3: 20° angle of damper flapper position with flow rate of 0.00014m³/s on the left and 0.000162m³/s on the right	54
Figure 4.4: Damper flapper with increasing angles	54
Figure 4.5: The location of the air pockets	58
Figure 5.1: Comparison of Turbulence Intensities (%) Before (Left) and After (Right) Damper Flapper Failure for 0° (Vertical) Angled Damper Flappers	60
Figure 5.2: Comparison of Turbulence Intensities (%) Before (Left) and After (Right) Damper Flapper Failure for 45° Angled Damper Flappers	61

CHAPTER 1

INTRODUCTION

This chapter provides an overview of the Final Year Project background, problem statement, objectives, scope of study, literature review, methodology and findings. The project requires the author to design and modify the test rig and seeks the possible root cause and accordingly, recommends methods or solutions to avoid reoccurrence by the end of the project.

1.1 Background.

Ethylene Ployethylene Malaysia Sdn Bhd (EPEMSB) is a petrochemical plant producing polyethylene. Part of the production process requires the cracking of ethane in a furnace. This furnace is equipped with an induction fan to create an artificial draught to facilitate the cracking process.

The induction fan on furnace F-102 failed along its cowling suspected due to high vibrations as a result of a broken cotter pin on one of the four damper flappers. The flow pattern of the artificial draught was distorted causing an induced turbulence and hence vibrations well above danger level

The furnace F-102 was out of service for 5 days. The root cause of its failure was not determined when it is out of service and F-102 was reinstated after the cotter pin, the induction fan and cowling were replaced.



Figure 1.1: Induction fan [6]



Figure 1.2: Cowling [6]

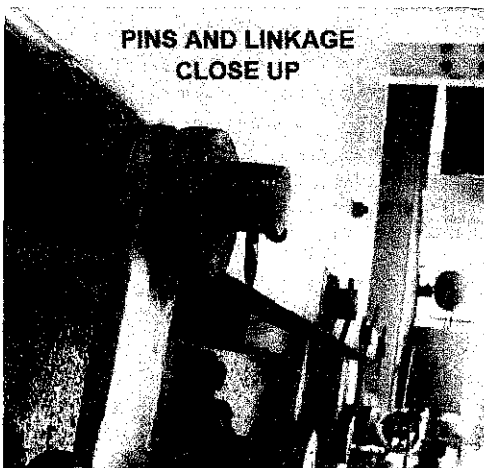


Figure 1.3: Cotter pin and linkage close up [6]

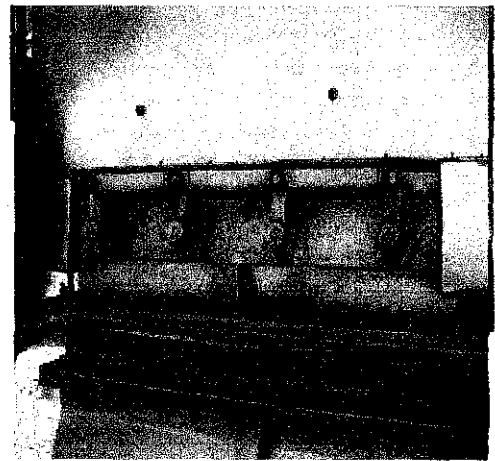


Figure 1.4: Assembly of cotter pins and linkage [6]

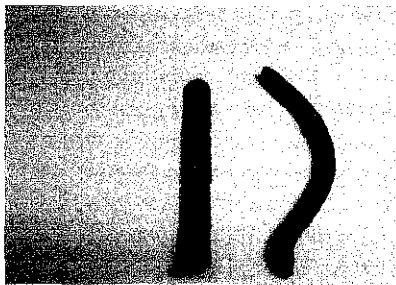


Figure 1.5: Broken cotter pin [6]

1.2 Problem statement.

Ethylene Polyethylene Malaysia Sdn Bhd (EPMSB) is a petrochemical plant producing polyethylene. To produce this material, one of the stages is the cracking of ethane into ethylene by heating the ethane in a furnace. An induction fan is used to create a draught in the furnace. However, the fan failed at one particular instance with the expected cause to be induced turbulence. Any interruption due to high induced turbulence will cause a large amount of production losses since any activity to troubleshoot the root cause is time demanding. A model of a furnace top shall be fabricated to simulate the flow in the furnace top section.

1.3 Objective.

- 1) Modifying an existing furnace top section.
- 2) Conduct an experiment to visualize the flow in a furnace top. Analyze and make a hypothesis based on the flow visualize in a top furnace.
- 3) Determine the probable root cause of high induce turbulence in the furnace top.

1.4 Scope of the study.

This experiment involve the designing and fabrication of furnace top or test rig, calculation for driver and pump requirements and material procurement. The literature review that involves this experiment includes laminar and turbulent flows, friction drags, dimensional analysis, the continuity equation, the ideal gas, and flow visualization using screens. The flow that will be visualize in the test rig will be analyze and make a hypothesis based on the flow patterns.

The outcome of this experiment is to determine the effect and the root cause of the induced turbulent. Note that this is a continuation of a previous FYP. From the previous experiment, one of the problems encountered is the leaking within the test rig. So to overcome this problem, the author proposes to use shims and gaskets assembled between each section of the test rig assembly. Also for the pump, it is shall to select a better pump for a good driver to conduct the experiment.

CHAPTER 2

LITERATURE REVIEW

This chapter contains the summarized version of the literature review study throughout the year. Hypotheses are formulated as a basis for the experimental modelling solely from the information gathered.

2.1 Ethane cracking furnace.

This part will discuss the brief description of the furnace, ethane and cracking process. Brief description is only as a simple as short description.

2.1.1 Brief description of the furnace.

A furnace is always referred to as a device that used for heating. According to American English, the term furnace is used to describe as household heating systems based on a central furnace. From British English the term furnace is described as mean industrial furnaces which are used for many things, such as the extraction of metal from ore (smelting) or in oil refineries and other chemical plants, for example as the heat source for fractional distillation columns. The term furnace can also refer to a direct fired heater, used in boiler applications in chemical industries or for providing heat to chemical reactions for processes like cracking, and are part of the Standard English names for many metallurgical furnaces worldwide. [1]

For this project, it is more to the industrial furnace. The industrial furnace is divided by 6 sections which are described later. The industrial furnace or direct fired heater is equipment used to provide heat for a process or reactor that provides heats of reaction. The design of the furnace varies according to its function, heating duty, type of fuel and method of introducing combustion air. Eventually all the furnaces have some common features. [1]

The operating principle of the furnaces can be described as follow. The fuel is introduced into the burner. The fuel mix with the air provided from an air blower and then the fuel-air mixture will burn. The flame from the combustion will heats up the tubes, which in turn heat the fluid (e.g. ethane) inside the first part of the furnace known as the radiant section. In the radiant section the heat is transferred to the tubes by mean of radiation. The heating fluid (e.g. ethane) will pass through the tubes and heat to the desired temperature 900°C or more. The resulting gases form the combustion is known as flue gas. The flues gas flow into the convection section where more heat is recovered. Then the flue gas vented to the atmosphere via flue gas stack with the help of an induced draft. [1]

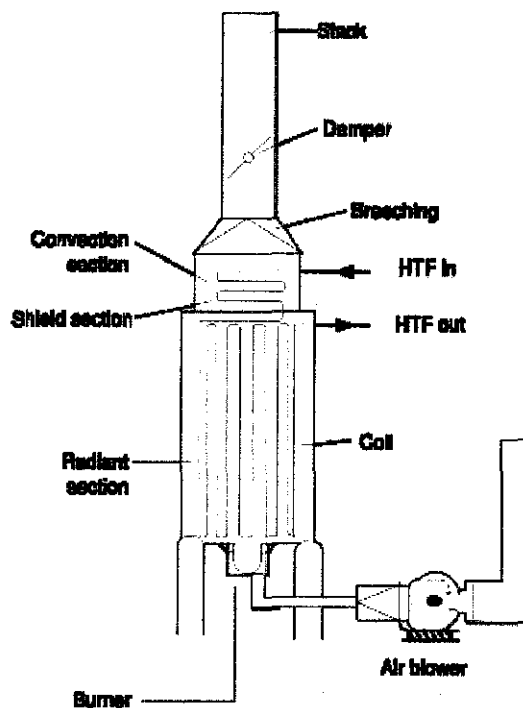


Figure 2.1: Industrial furnaces diagram. [17]

2.1.2 Brief description of ethane.

Ethane is a chemical compound with chemical formula C_2H_6 . It is the only two-carbon alkane, that is, an aliphatic hydrocarbon. At standard temperature and pressure, ethane is a colourless, odourless gas. Ethane is isolated on an industrial scale from natural gas, and as a by product of petroleum refining. Its chief use is as petrochemical feedstock for ethylene production. Ethane is the second-largest component of natural gas. The natural gas from different gas field varies in ethane content. Ethane can be separated from the other components of natural gas in most well-developed gas field. In Malaysia, the Resak field produce only the natural gas where the product from the well is a two phase product which is liquid and gas. The two phase liquid is retrieve to the surface and it flows into many separators by mean to separate it into gas, condensate and water. Ethane can be separated from this petroleum gas, a mixture of gaseous hydrocarbons and liquids that arise as a by-product of petroleum refining. Ethane can be separate from methane by liquefying it at cryogenic temperature (very low temperature, below $-150\text{ }^\circ\text{C}$). [2]

The main uses of ethane in the chemical industry are to produce the ethylene by steam cracking. The ethane will be diluted with the steam and heated to very high temperature, about 900°C or more. Heavy hydrocarbons break down into lighter hydrocarbons, where saturated hydrocarbons become unsaturated. Ethane is favourable for ethylene production because the steam cracking of ethane is fairly selective for ethylene.

2.1.3 Brief description of the cracking process.

The cracking process is a process where heavy hydrocarbons are broken down into simpler molecules. This process is used to produce a lighter hydrocarbon such as ethylene from the heavy hydrocarbons (e.g. ethane). In industry, they use the Naphtha, a crude oil fraction with composition between C_6 and C_{20} . [3] It is thermally cracked in a furnace at $900^{\circ}C$ or more to produce ethylene and propylene, the base chemicals for polyethylene and polypropylene. The rate of cracking depends on the temperature and presence of any catalysts. Cracking process also referred to as pyrolysis, the breakdown of a large alkane into smaller and more useful alkanes and alkenes.

When referring to the steam cracking, it is commonly used for cracking a gaseous or liquid hydrocarbon feed like Naphtha, LPG or ethane. This initial feed is diluted with steam and then briefly heated in a furnace, without the presence of oxygen, to a high temperature commonly at $900^{\circ}C$ or higher. Typically the reaction temperature is very hot but the reaction is only allowed to take place briefly. After the cracking temperature has been achieved, the gas is quickly being quenched to stop the reaction. [3]

The effectiveness of the reaction depends on the feed composition, ratio of hydrocarbon to steam and the cracking temperature. Ethane feed give product stream rich in lighter alkanes, ethylene. Naphtha feed give some of the light hydrocarbon product but also rich in aromatics hydrocarbons and hydrocarbons suitable for inclusion in gasoline or fuel oil. The high cracking temperature produces ethane and benzene favourably, while lower temperature produces higher amount of propene and liquid products.

2.2 Laminar flow.

The fluid flow in a duct may be laminar, transitional or turbulent. This kind of flow much depends on the flow rate or fluid energy. The flow transform from laminar to transitional and consequently turbulent flow with increasing flow rate. This kind of flow sometime known as streamlines flow. Laminar flow occurs when a fluid flow is in parallel layers, with no disruption between layers. Laminar flow is a flow regime characterized by high momentum diffusion, low momentum convection, pressure and velocity independent from time. In laminar flow, the Reynolds number is less than 2100. The extreme case of laminar flow is where viscous or friction effect is much greater than the inertial forces. This flow is called the creeping motion or Stokes flow, occurs when the Reynolds number is much less than 1. In general, the laminar flow is a well define flow. [4]

2.3 Transitional flow.

Transitional flow is a flow in which the viscous and Reynolds stresses are of approximately equal magnitude. It is transitional between laminar flow and turbulent flow. Transitional flow displays a general pattern, however, with several random disorders along the flow line. [5][4]

2.4 Turbulent flow.

Turbulent flow is in a disordered pattern. It is a flow regime characterized by chaotic form. This includes low momentum diffusion, high momentum convection and rapid variation of pressure and velocity in space and time. In turbulent flow, unsteady vortices appear on many scales and interact with each other. The drag, due to skin friction, is relatively high. As the flow rate increases, it will increase the turbulence. Turbulence also creates eddies with different length scale. [4]

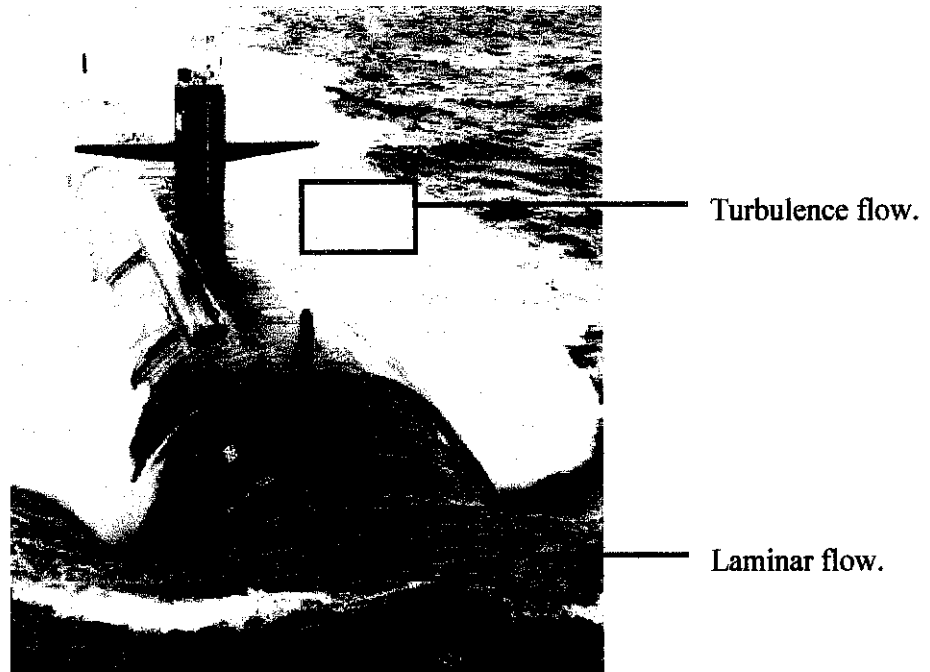


Figure 2.2: Laminar and turbulent water flow over the hull of a submarine. [18]

2.5 Friction drag.

Any object moving through a fluid will experience a drag. A drag is induced by pressure and shear forces on the surface of an object moving through a fluid. This is a combination of flow direction components of the normal and tangential forces on the body. Typically, the result for a given shaped object is a drag coefficient, C_D , where

$$C_D = \frac{D}{\frac{1}{2}\rho U^2 A}$$

Friction drag, D_f , is that part of the drag that is due directly to shear stress, τ_w , on the object. It is a function of not only the magnitude of the wall shear stress, but also of the orientation of the surface on which it acts. Friction drag depends on the orientation of the body as well as the magnitude of the wall shear stress τ_w . Most of the drag flows with low Reynolds number, usually due to friction. [4][6]

2.6 Pump type.

This section only will describe the centrifugal and axial flow pump only since there is a need to make a comparison between them.

Axial Flow Pump (AFP).

An axial flow pump is a common type of water pump that essentially consists of a propeller in a tube. The propeller can be driven directly by a sealed motor in the tube or by a right-angle drive shaft that pierces the tube. The main advantage of an AFP is that it can easily be adjusted to run at peak efficiency at low-flow/high-pressure and high-flow/low-pressure by changing the pitch on the propeller. These pumps have the smallest of the dimensions among any of the conventional pumps and are more suited for low heads and higher discharges. An application example of an AFP would be transfer pumps used for sailing ballast.

Within Axial Flow Pumps, the impeller pushes the liquid in a direction parallel to the pump shaft. Axial flow pumps are sometimes called propeller pumps because they operate essentially the same as the propeller of a boat. The impeller of a typical axial flow pump and the flow through a radial flow pump are shown in the illustration below.

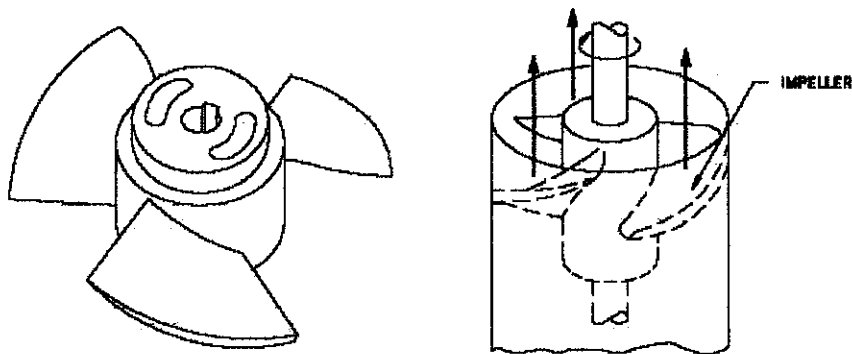


Figure 2.3: Axial flow pump propeller. [19]



Figure 2.4: Model AF/MPAF Axial Flow Pump. [7]

Specifications of Axial Flow Pump:

- 1) Capacities to 200,000 GPM (9.7222 m³/s).
- 2) Heads to 30 feet (9 m).
- 3) Temperatures to 600° F.
- 4) Pressures to 150 PSIG (1034 kPa).
- 5) Solids to 9 in. (228 mm).

Reference: <http://www.gouldspumpsashland.com/Axial-Flow-Pump.htm>.

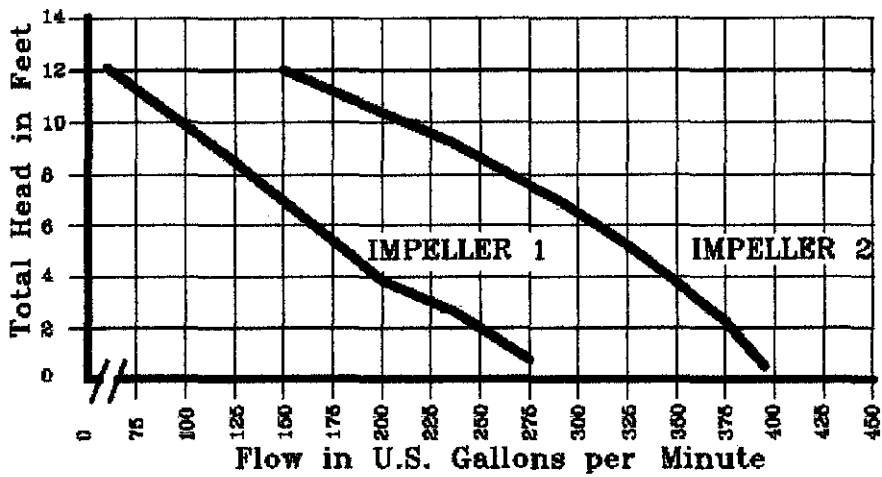


Figure 2.5: Typical axial flow pump performance curve. [8]

Advantages:

- 1) Strong.
- 2) Versatile.
- 3) Simple design and construction.
- 4) Wide range of pressures.
- 5) Higher discharge pressures than centrifugal pumps for less power consumption.
- 6) Better suction lift than centrifugal pumps.
- 7) To 20% more efficient than centrifugal pumps.
- 8) Self-priming.
- 9) Accurate volume control.

Disadvantages:

- 1) More expensive to buy than centrifugal pumps.
- 2) More moving parts requiring more maintenance.
- 3) Expensive to repair.
- 4) Not good for abrasive liquids.
- 5) The liquid in the discharge line has pulses of pressure.
- 6) Too many moving parts to operate well at high speeds.
- 7) Need to have Pressure Relief Valves (PRV) fitted.

Centrifugal Pumps.

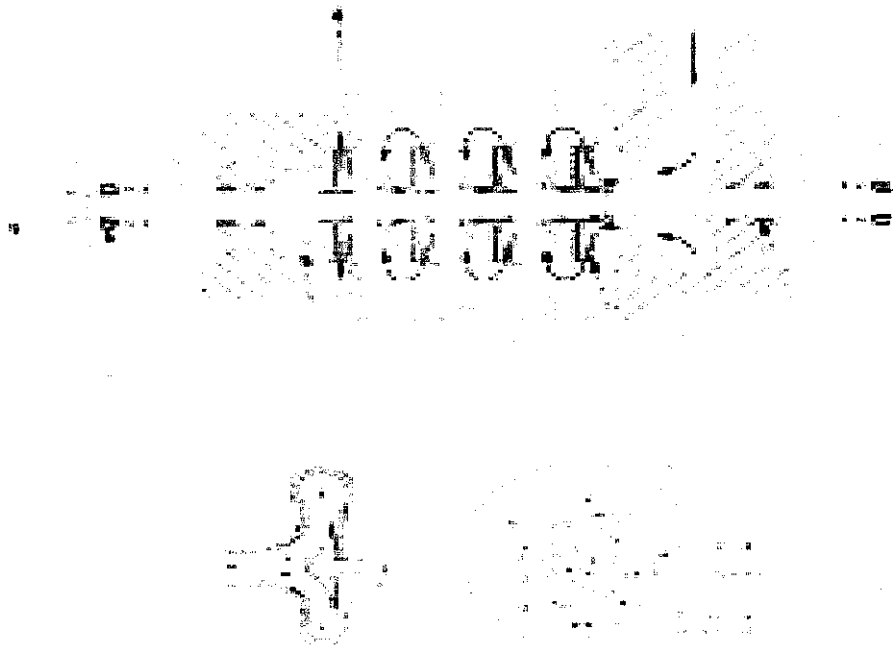


Figure 2.6: A schematic of a typical centrifugal pump. [9]

A centrifugal pump adds kinetic energy to a fluid by means of fast-rotating impellers. There is no fixed volume, and the fluid increases in kinetic energy (velocity) while moving through impeller passages by centrifugal force resulting from impeller rotation. Its accelerated velocity is converted into pressure head by exiting into the diffuser for discharge, or - in the case of a multi-stage centrifugal pump - it further increases its velocity (pressure head) by moving through to the next fast-rotating impeller. Centrifugal pumps are usually direct coupled with drivers (electric motors or engines) without speed reduction. [9]

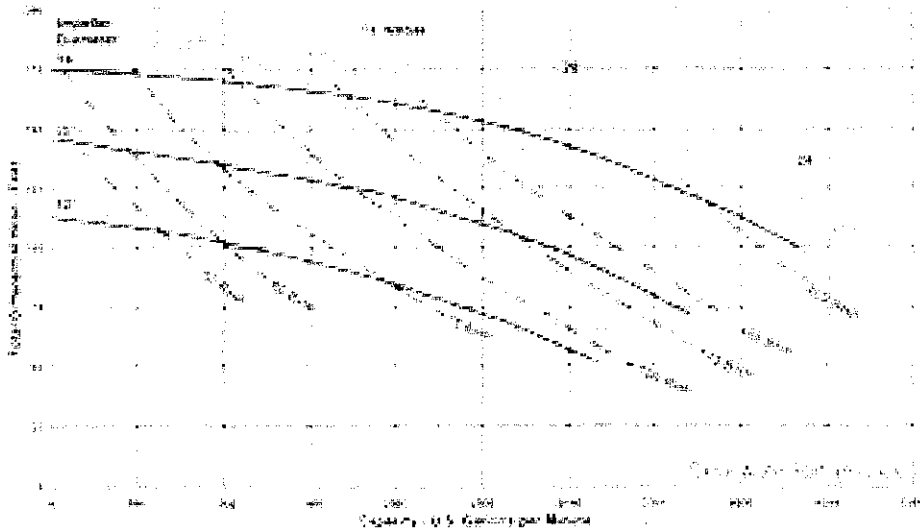


Figure 2.7: A typical performance curve of a centrifugal pump. [10]

Centrifugal Pump.

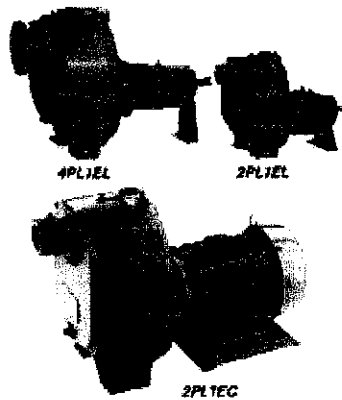


Figure 2.8: Model Prime Line® Centrifugal Pump. [9]

Specifications of Prime Line® Centrifugal Pump:

- 1) Sizes 2" (51 mm) through 12" (305 mm).
- 2) Capacities to 7,000 GPM (0.4444 m³/s).
- 3) Heads to 250 feet (76 m).
- 4) Temperature to 200° F (94° C).
- 5) Suction Lifts to 25 feet (7.6 m).
- 6) Solids Handling to 3" (76 mm).

Reference: <http://www.gouldspumpsashland.com/Centrifugal-Pump.htm>.

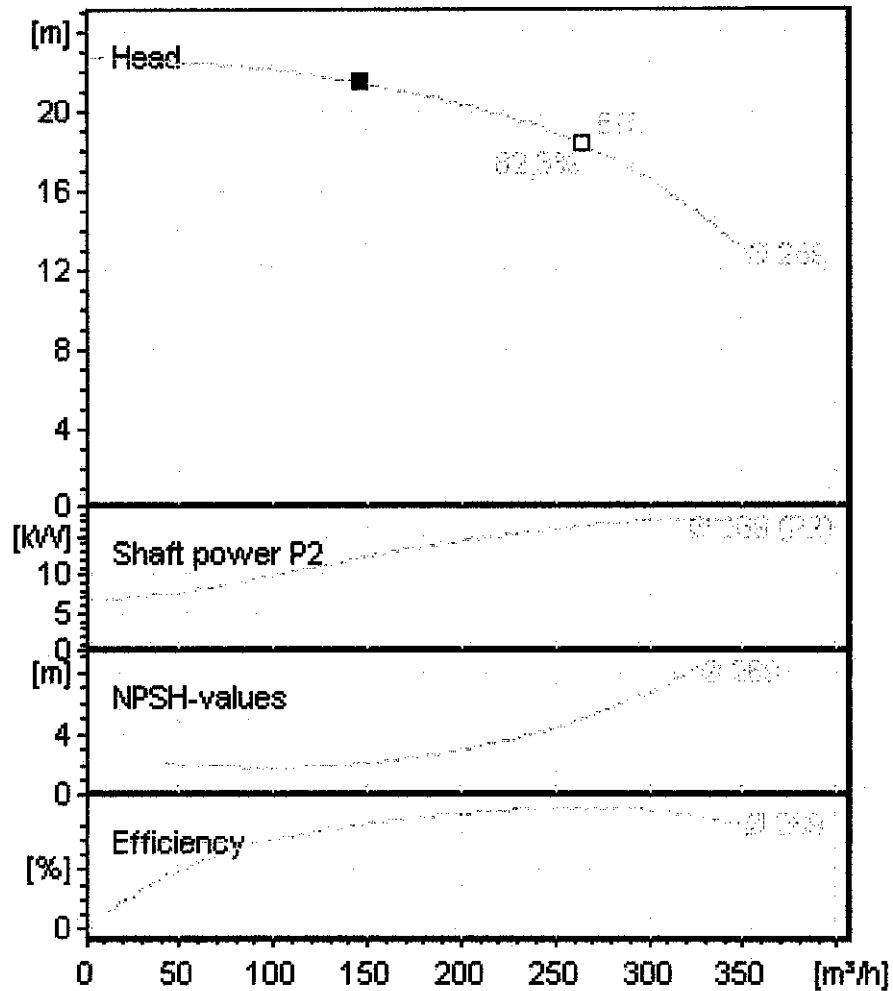


Figure 2.9: Typical performance curve of a centrifugal pump. [10]

Since a centrifugal pump has no fixed volume (as indicated above) at a fixed inlet size and casing, increasing the diameter of the impeller or the rotational speed will lead to increased head and increased flow rate. A centrifugal pump can have a large capacity with a small footprint compared with a reciprocating pump. Of course, increased capacity will consume more energy. Capacity is proportional to impeller speed and diameter. Larger impeller diameter (higher exit velocity) and/or faster rotation speed will increase the head due to conversion of velocity to head. Head is proportional to the square of the impeller diameter or speed. Further increase of head could also result from more stages of impellers. More stages also mean more friction loss between inlet and outlet. [10]

The overall efficiency on a centrifugal pump normally ranges from 30 percent to 60 percent depending on pump design and system operating parameters vs. pump performance parameters. This results from pump over-sizing and considerations of system flow rate/head safety margins when the system is designed or the system operating parameters change. [10]

Efficiencies up to 85 percent can be reached on special designs which operate at BEP (best efficiency point) when pump performance curve and system-operating curve match perfectly. [10]

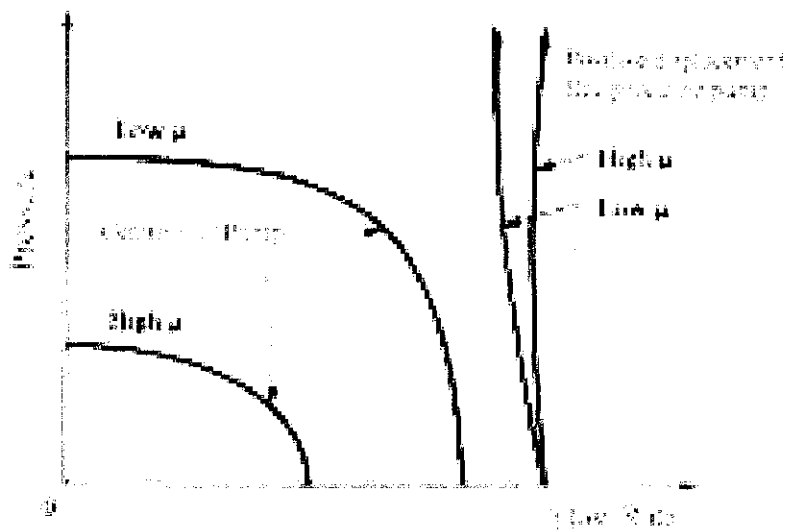


Figure 2.10: Comparison of performance curves of typical centrifugal reciprocating pumps at constant speed. [10]

2.7 Dimensional Analysis.

There is a certain aspect of this important engineering tool that must seem a little baffling and mysterious. It is the matter of the selection of variables. Geometry, material properties and external effects are the variables that need to be considered. According to Franzini and Finnermore, there are three conditions to be fulfilled for complete similarity to be achieved. [4][6]

- 1) Geometric similarity-the model must have the same shape as the prototype only differing in geometric scale.
- 2) Kinematics similarity-velocities at any point in the model must be proportional to the corresponding point in the prototype by a scale factor.
- 3) Dynamic similarity-all forces in the model must be in ratio with the corresponding forces in the prototype.

2.7.1 Reynolds Number.

In fluid mechanics, the Reynolds number is the ratio of inertial forces ($v_s\rho$) to viscous forces (μ/L) and consequently it quantifies the relative importance of these two types of forces for given flow conditions.

The Reynolds Number generally of importance in all types of fluid dynamics problems. [4]

It is one of the most important dimensionless numbers in fluid dynamics and is used, usually along with other dimensionless numbers, to provide a criterion for determining dynamic similitude. When two geometrically similar flow patterns, in perhaps different fluids with possibly different flow rates, have the same values for the relevant dimensionless numbers, they are said to be dynamically similar, and will have similar flow geometry.

The Reynolds Number also used to identify the different flow regimes, such as laminar or turbulent flow. Turbulent flow occurs at high Reynolds numbers while laminar flow occurs at low Reynolds numbers.

$$\text{Re} = \frac{\text{Inertial Forces}}{\text{Viscous Forces}} = \frac{\rho v_s L}{\mu} = \frac{v_s L}{\nu}$$

v_s - Mean fluid velocity, [m s^{-1}]

L - Characteristic length, [m]

μ - (Absolute) dynamic fluid viscosity, [N s m^{-2}] or [Pa s]

ν - Kinematics fluid viscosity: $\nu = \mu / \rho$, [$\text{m}^2 \text{s}^{-1}$]

ρ - Fluid density, [kg m^{-3}]

2.7.2 Mach Number.

The Mach number is the ratio of the fluid speed to the speed of sound in the fluid [4]. It is a dimensionless measure of relative speed. Mach number is the number of times the speed of sound an object or a duct, or the fluid medium itself, moves relative to each other. It is named after Austrian physicist and philosopher Ernst Mach. The Mach number application is where a flow in which the compressibility of the fluid is important. [6]

$$Ma = \frac{V}{c}$$

V= velocity of the object relative to the medium.

c= velocity of sound in the medium.

2.7.3 Prandtl Number.

The Prandtl number is a dimensionless number approximating the ratio of momentum diffusivity (viscosity) and thermal diffusivity. It is named after Ludwig Prandtl.

Typical values for Pr are:

- 1) Around 0.7 for air and many other gases.
- 2) Around 7 for water.
- 3) Around 7×10^{21} for Earth's mantle.
- 4) Between 100 and 40,000 for engine oil.
- 5) Between 4 and 5 for R-12 refrigerant.
- 6) Around 0.015 for mercury.

When Pr Number is small, it means that the heat diffuses very quickly compared to the velocity (momentum). This means that for liquid materials the thickness of the thermal boundary layer is much bigger than the velocity boundary layer. [6]

$$Pr = \frac{\text{MomentumBoundaryLayerThickness}}{\text{ThermalBoundaryLayerThickness}} = \frac{\text{ViscousDiffusionRate}}{\text{ThermalDiffusionRate}} = \frac{\nu}{\alpha}$$

ν = kinematics viscosity, $\nu = \mu / \rho$ [Pa s m³ kg⁻¹].

α = thermal diffusivity, $\alpha = k / (\rho c_p)$ [m² S⁻¹].

2.7.4 Nusselt Number.

The Nusselt number is a dimensionless number that measures the enhancement of heat transfer from a surface that occurs in a 'real' situation, compared to the heat transferred if just conduction occurred. It is named after Wilhelm Nusselt, a German engineer. Typically, the Nusselt number (Nu) it is used to measure the enhancement of heat transfer when convection takes place. [6]

$$Nu_L = \frac{hL}{k_f} = \frac{\text{ConvectionHeatTransfer}}{\text{ConductiveHeatTransfer}}$$

L=characteristic length (m).

k_f =thermal conductivity of the fluid (W/m.K).

h=convection heat transfer coefficient (w/m².K).

2.8 The Continuity Equation.

The continuity equation is simply an expression of the principle of conservation of mass. For a control volume the mass flow rate of the fluid into the control volume must equal that of the fluid leaving the control volume [6]. A 'continuity equation is a differential equation that describes the conservative transport of some kind of quantity. Since mass, energy, and momentum are conserved, a vast variety of physics may be described with continuity equations.

$$\sum m_{in} = \sum m_{out}$$

$$(\rho AV)_{in} = (\rho AV)_{out}$$

Assuming the density of the flow remains constant, the equation can be simplified as below:

$$Q = AV_1 = AV_2 \quad Q = \text{flow rate of the fluid.}$$

This equation is called the continuity equation for steady one-dimensional incompressible flow. In steady flows, the properties of a fluid at one particular point do not change with respect to time. Below is the continuity relationship for a compressible flow. For gases of high velocity flows, the flow is compressible and thus the values of specific gravity with pressure will differ causing an increase of the mass within the control volume with respect to time. [4][6]

$$\frac{\partial}{\partial t} \int_{cv} \rho dV + \sum \rho_{out} A_{out} V_{out} - \sum \rho_{in} A_{in} V_{in} = 0$$

2.8.1 Venturi.

A venturi is a flow meter with 3 sections in which the first being the main duct, the second a narrow section and the third being a wide section. From the continuity equation it was established that $Q = A_1 v_1 = A_2 v_2$ (for an incompressible flow). In a venturi, the decrease in area from the main duct to the throat causes the fluid to accelerate at the second section and consequently decelerate upon entering the divergent third section. The kinetic cross sectional area and vice versa with enlarged cross sectional area. [6]

2.9 The Ideal Gas.

Gases are highly compressible in comparison to liquids, with changes in gas density directly related to changes in pressure and temperature through the equation.

$$p = \rho RT$$

p = absolute pressure.

ρ = density.

T = absolute temperature.

R = gas constant.

The equation above commonly termed the perfect or ideal gas law. To understand the properties of real gases, a hypothetical gas known as the ideal gas is used to describe the relationship between the pressure, volume and temperature of the gas. [4][6]

2.9.1 Properties of Ideal Gases.

- 1) All collisions of molecules are perfectly elastic. Therefore, all the internal energy is in the form of kinetic energy and any change in internal energy is accompanied by a change in temperature.
- 2) The volume occupied by the molecules is insignificant with respect to the volume occupied by the gas.
- 3) There are no attractive or repulsive forces between molecules or between the molecules and the walls of the container. [6]

Ideal gas law

$$PV = nRT = NkT$$

n=number of moles.

$$R=\text{universal gas constant}=8.3145 \frac{J}{mol.K}$$

N=number of molecules.

$$k=\text{Boltzmann constant}=1.38066 \times 10^{-23} \frac{J}{k} = 8.617385 \times 10^{-5} \frac{eV}{K}$$

$$k = \frac{R}{NA}$$

$$NA=\text{Avagadro's number} = \frac{6.0221 \times 10^{23}}{mol}$$

2.9.2 Dalton's Law.

In chemistry and physics, Dalton's law (also called Dalton's law of partial pressures) states that the total pressure exerted by a gaseous mixture is equal to the sum of the partial pressures of each individual component in a gas mixture. This empirical law was observed by John Dalton in 1801 and is related to the ideal gas laws. In the case of a mixture of ideal gases, Dalton's Law of partial pressures state that the total pressure exerted by a mixture is equal to the sum of the pressure exerted by the components of the gas. It is also known as the law of additive pressures for obvious reasons. [6]

$$P_a = \frac{naRT}{V}$$

$$P_b = \frac{nbRT}{V}$$

$$P_c = \frac{ncRT}{V}$$

.....

Thus

$$p = p_a + p_b + p_c + \dots$$

And

$$p = \frac{RT}{V} \sum n$$

$$P_j / p = y_j$$

2.9.3 Amangat's Law.

Amangat postulated that the total volume occupied by a gas mixture is equal to the sum of the volumes that the pure components would occupy at the same pressure and temperature and hence, analogous in additive volumes with that of additive pressures for Dalton's Law. [6]

$$V_a = \frac{naRT}{P}$$

$$V_b = \frac{nbRT}{P}$$

$$V_c = \frac{ncRT}{P}$$

.....

Thus

$$V = V_a + V_b + V_c + \dots$$

$$V = \frac{RT}{P} \sum \dot{n}$$

$$V_j / v = y_j$$

2.9.4 Apparent Molecular weight and Specific Gravity of Gases in a Mixture.

When dealing with a mixture of gases, the apparent molecular weight is the summation of the partial molecular weights contributed by each component in the mixture expressed as:

$$M_a = \sum y_j M_j$$

The specific gravity (γ) of gas is defined as the ration of the density of the gas in question to that of the density of air at the same temperature and pressure.

[6]

$$\text{Gravity, } g = \frac{\rho_{gas}}{\rho_{air}} = \frac{M_{gas}}{M_{air}} = \frac{M_{gas}}{29}$$

$$\gamma_{gas} = g \times \rho_{air}$$

2.10 Flow in Non-Circular Conduits.

Calculations for fully developed turbulent flow in ducts of noncircular cross section are usually carried out by using the Moody chart data. But it is only relevant for round pipes. Not all ducts are circular and thus a slight modification is necessary to obtain parameters such as the Reynolds number and, major and minor losses. For turbulent flow such calculations are usually

accurate to within about 15%. Practical, easy to use results can be obtained by introducing the hydraulic diameter. [14][6]

$$D_h = 4A / P$$

Defined as four times the ratio of the cross sectional flow area divided by the wetted perimeter, P , of the pipe. The hydraulic diameter is also used in the definition of the friction factor,

$$h_L = f(\ell / D_h) \bar{V}^2 / 2g$$

the Reynold number,

$$Re_h = \frac{\rho V D_h}{\mu}$$

and the relative roughness.

$$\frac{\varepsilon}{D_h}$$

2.11 Honeycombs and Screens.

Honeycombs are arrays of hexagonal tubular arranged parallel to one another and are generally used as flow directionalizers-stabilizers and/or to reduce lateral components of turbulence in a flow. A honeycomb naturally produces some turbulence of its own. With eddy sizes of the same order as the cell diameter, which decays very much slowly than that of which created by screens. The honeycomb is best placed just upstream of the test section to streamline the flow. [6][11]

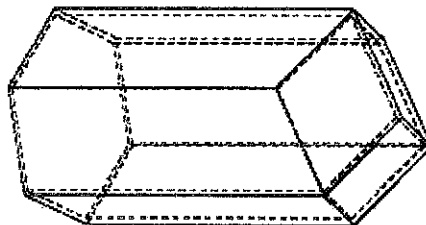


Figure 2.11: The three-dimensional geometry of a honeycomb cell. [20]

2.12 Centre of Mass.

The centre of mass of a system is defined as the specific point in which the systems' mass behaves as if it were concentrated. On one plane, that is like the balancing of a see-saw about a pivot point with respect to the torques produced.

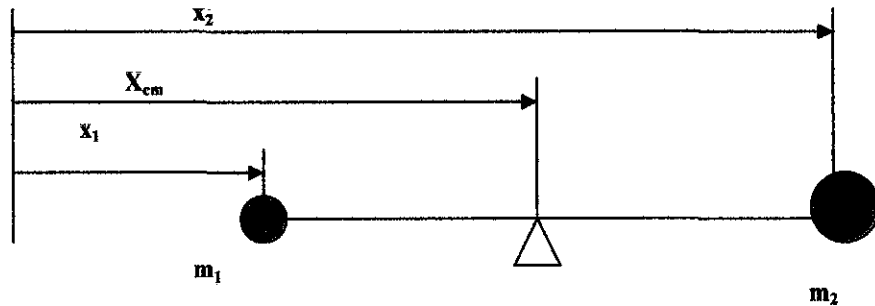


Figure 2.12: Centre of mass illustration.

$$X_{cm} = \frac{m_1 x_1 + m_2 x_2}{m_1 + m_2}$$

In physics, the center of mass of a system of particles is a specific point at which, for many purposes, the system's mass behaves as if it were concentrated. The center of mass is a function only of the positions and masses of the particles that comprise the system. The center of mass of a body does not always coincide with its intuitive geometric center, and one can exploit this freedom. [6]

2.13 Torque Sequences.

The torque sequence is applied when tightening the bolts and nuts for each compartment assembly. If one or more screws, bolts, or nuts of a series are tightened, as in a series of bolts around a flange or a half-shell, all of that series must be tightened equally to prevent distortion, damage, or leakage. See Figure for torque sequences for bolt patterns. [12]

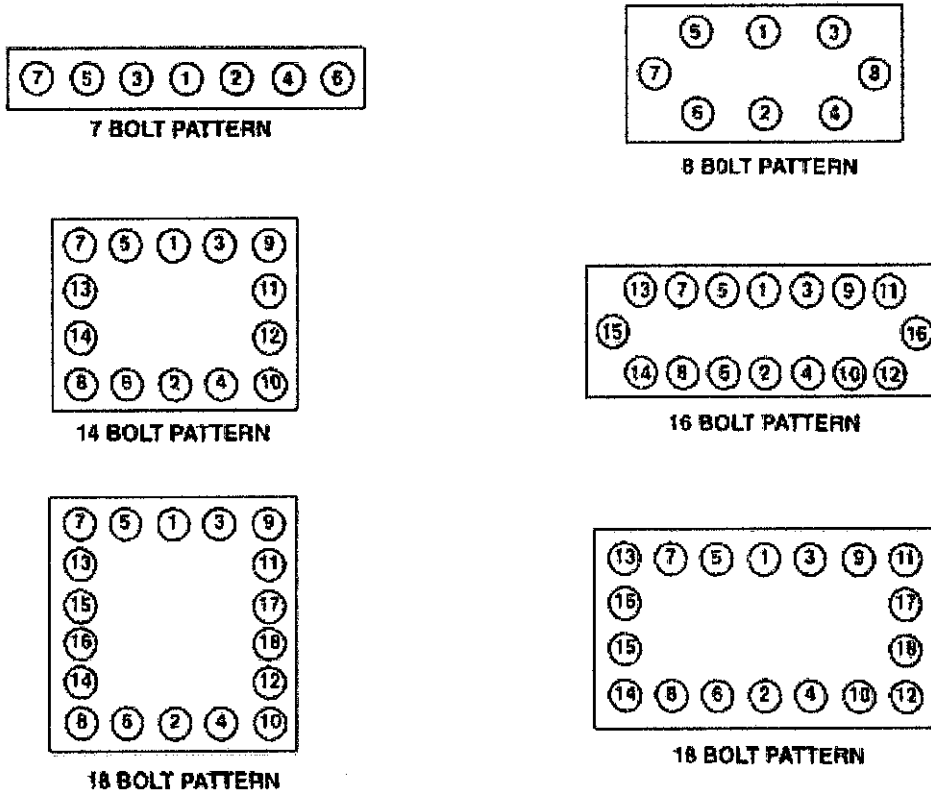


Figure 2.13: Torque sequences for bolt patterns. [12]

2.14 Manometer.

Manometers measure a pressure difference by balancing the weight of a fluid column between the two pressures of interest. A common simple manometer consists of a U shaped tube of glass filled with some liquid. Typically the liquid is mercury because of its high density

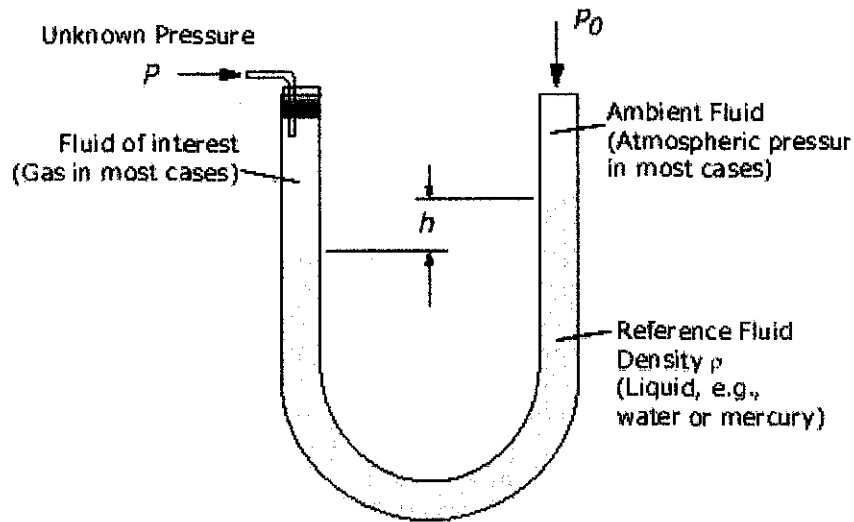


Figure 2.14: Illustration of a basic manometer design [13].

The pressure difference between the bottom and top of an incompressible fluid column is given by the incompressible fluid static equation,

$$\Delta P = P - P_o = \rho g h$$

where $g = 9.81 \text{ m/s}^2$.

There are 3 fundamental cases that need to be considered when dealing with U shaped manometer. These 3 cases will be discussed as follow.

Case 1.

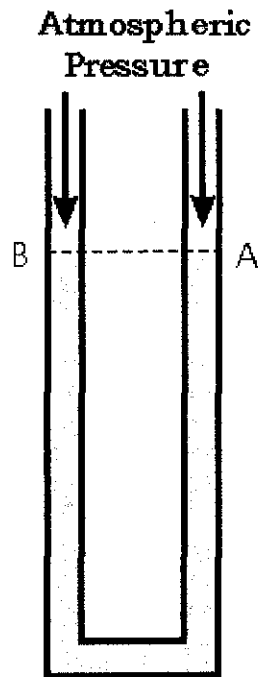


Figure 2.15: U-shaped manometer with both end open to the atmosphere [14].

The figure show such a U-shaped manometer filled with a liquid. From the figure we can see that both end of the tube are open to the atmosphere. This indicates that the point A and B are at atmospheric pressure. The points also have the same vertical height. [14]

Case 2.

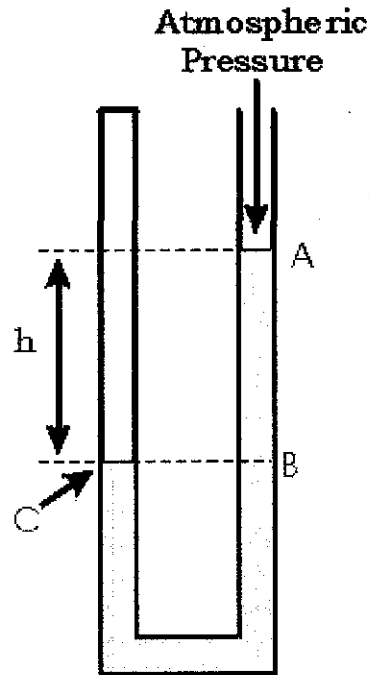


Figure 2.16: U-shaped manometer with one closed end [14].

Now the top of the tube on the left has been closed while the right side of the tube remain open to the atmosphere. We imagine that there is a sample of gas in the closed end of the tube. We can see straight away that point A is at atmospheric pressure. The point C exhibit the pressure of the gas in the closed end of the tube. The point B has a pressure greater than atmospheric pressure. The point C is at the same height as B, so it has the same pressure as B. Thus, in this case the pressure of the gas that is trapped in the closed end of the tube is greater than atmospheric pressure. [14]

Case 3.

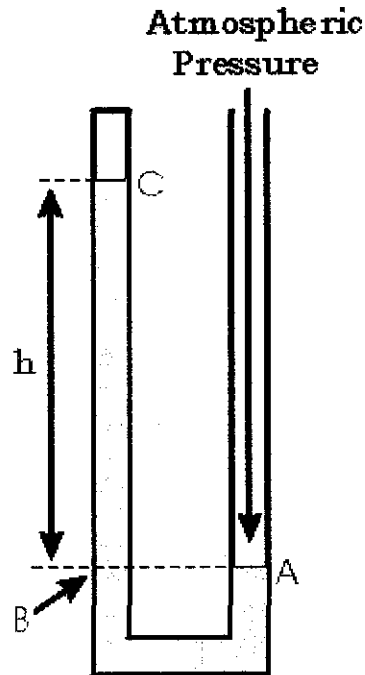


Figure 2.17: U-shaped manometer with one closed end [14].

Now we show another possible arrangement of the manometer with the top of the left side of the tube closed. Perhaps the closed end of the tube contains a sample of gas as before, or perhaps it contains a vacuum. The point A is at atmospheric pressure. The point C is at the pressure of the gas in the closed end of the tube has, or if the closed end contains a vacuum the pressure is zero. The point B also at the atmospheric pressure since it is at the same height of point A. The pressure at B is also the sum of the pressure at C plus the pressure exerted by the weight of the column of liquid of height h in the tube. We conclude that pressure at C, then, is less than atmospheric pressure by the amount of pressure exerted by the column of liquid of height h . If the closed end of the tube contains a vacuum, then the pressure at point C is zero, and atmospheric pressure is equal to the pressure exerted by the weight of the column of liquid of height h . In this case, the manometer can be used as a barometer to measure atmospheric pressure. [14]

In many situations, measuring pressures in units of length of the liquid in the manometer is perfectly adequate. The remainder of this document discusses how to convert from those units to pascals. The figure below shows a cylinder of liquid of height h and area A . The weight of the cylinder is its mass m times the acceleration due to gravity g . This is the force exerted by the cylinder of liquid on whatever is just below it: [14]

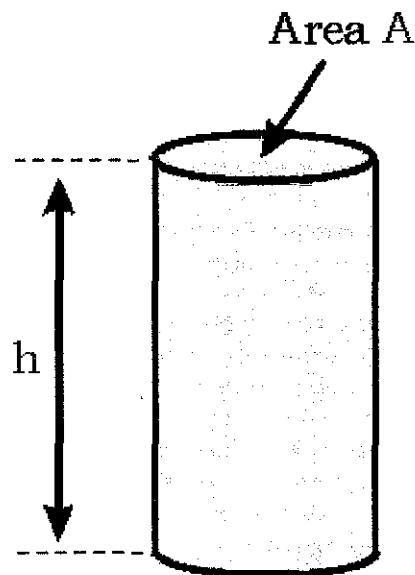


Figure 2.18: A cylinder illustration for deriving the pressure equation [14]

$$F = mg$$

The pressure p is this force divided by the area A of the face of the cylinder.

$$p = \frac{F}{A}$$

The mass of the cylinder is the density of the liquid times the volume V .

$$m = \rho V$$

The volume is the area A of the face of the cylinder times its height h .

$$V = Ah;$$

$$p = \frac{F}{A}$$

$$p = \frac{mg}{A}$$

$$p = \frac{\rho Vg}{A}$$

$$p = \frac{\rho Ahg}{A}$$

$$p = \rho gh$$

$$V = A h \quad [14]$$

2.15 Flue gas stacks draft.

The combustion flue gases inside the flue gas stacks are much hotter than the ambient outside air and therefore less dense than the ambient air. That causes the bottom of the vertical column of hot flue gas to have a lower pressure than the pressure at the bottom of a corresponding column of outside air. That higher pressure outside the chimney is the driving force that moves the required combustion air into the combustion zone and also moves the flue gas up and out of the chimney. That movement or flow of combustion air and flue gas is called "natural draft (or draught)", "natural ventilation", "chimney effect", or "stack effect". The taller the stack, the more draft (or draught) is created.

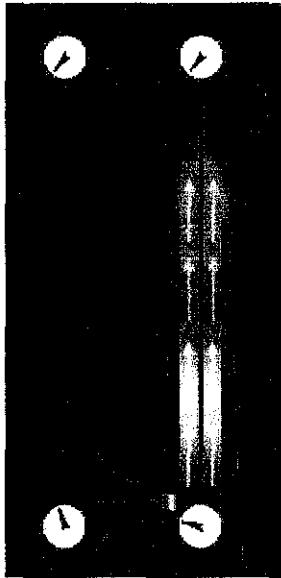


Figure 2.19: The stack effect in chimneys: the gauges represent absolute air pressure and the airflow is indicated with light grey arrows. The gauge dials move clockwise with increasing pressure. [21]

CHAPTER 3

METHODOLOGY

3.1 Description of the methodology used in the study.

This Final Year Project (FYP) starts from semester 1 until semester 2. The main gist of this FYP is to modify the existing model of a furnace top. To ensure that this project runs smoothly and successfully, it has been divided into 2 major parts. For the first part, will be done on the 1st semester, is the conceptual and literature review such as laminar and turbulent flow, friction drags, dimensional analysis, the continuity equation, the ideal gas concept, designing the test rig using AutoCAD and pump types and requirements. This is basically a study and research of fundamental and theoretical review conducted via searching through journals, websites and related articles and text books. For the 2nd part, this is conducted on the second semester, where it involve the fabrication of the modified furnace top or test rig, driver and pump requirements, material procurements and last but not least, an experiment for flow visualization in the test rig or furnace top. Initially the furnace top was design using the AutoCAD software. It will show all the necessary engineering drawing of the test rig. This test rig was design into several sections, outlet nozzles, main compartment, diffuser section and inlet section. The reason the test rig was design this way is to ease the fabrication of the test rig. The shims or gaskets will be installed between the test rig assemblies. After the fabrication was done, an experiment will be conduct to visualize the flow in the furnace top. From the flow visualization, it will be analyze and make a hypothesis from the flow. Then the determination of a probable root of high induce turbulence in the furnace top will be conducted.

3.2 Dimensional similarity.

The model has been scaled down to 1/10th of the original furnace top geometry. In computing the inlet velocities of the furnace top several assumptions made as follows:

- 1) The flue gas flow within the furnace is incompressible. (**APPENDIX I**)
- 2) The flow has achieved a steady state.
- 3) No heat exchange between the hot flue gas and the surroundings.
- 4) The flue gas abides by the Ideal Gas Law.
- 5) Flue gas released as a by product of complete combustion.

There must be a suitable medium of fluid for the test rig to be selected as a substitute for air in the original furnace top. From the calculation shown in **APPENDIX I**, the low kinematic viscosity medium, water, will generate an inlet and outlet velocity of 1.623 m/s and 2.97 m/s respectively. The model cannot be scaled down any further to avoid higher velocities that would make it impossible for flow visualization and may cause the test section to fail due to high pressure.

The continuity equation, based on the above assumptions, used to compute the outlet and inlet velocities from the flow rate and area measurements provided. This is due to unavailability of the real inlet and outlet velocities of the furnace top. An incompressible flow was confirmed once the Mach number indicated that the flow at both inlet and outlet of the furnace top was incompressible at 0.0202.

3.3 Designing the test rig.

The test rig was designed using Computer Aided Software (CAD) code AutoCAD for the 2D and 3D drawing. The model was scaled down to 1/10th of the original geometry of the furnace top with maximum height of 1.0 m and maximum combined length of 0.35 m

3.3.1 Engineering Drawings.

In this section, the orthographic drawing of main compartment, diffuser compartment, damper flapper compartment, outlet nozzle and water container. The 3D drawings also illustrated in this section.

Orthographic drawings of Test Section (in compartments)

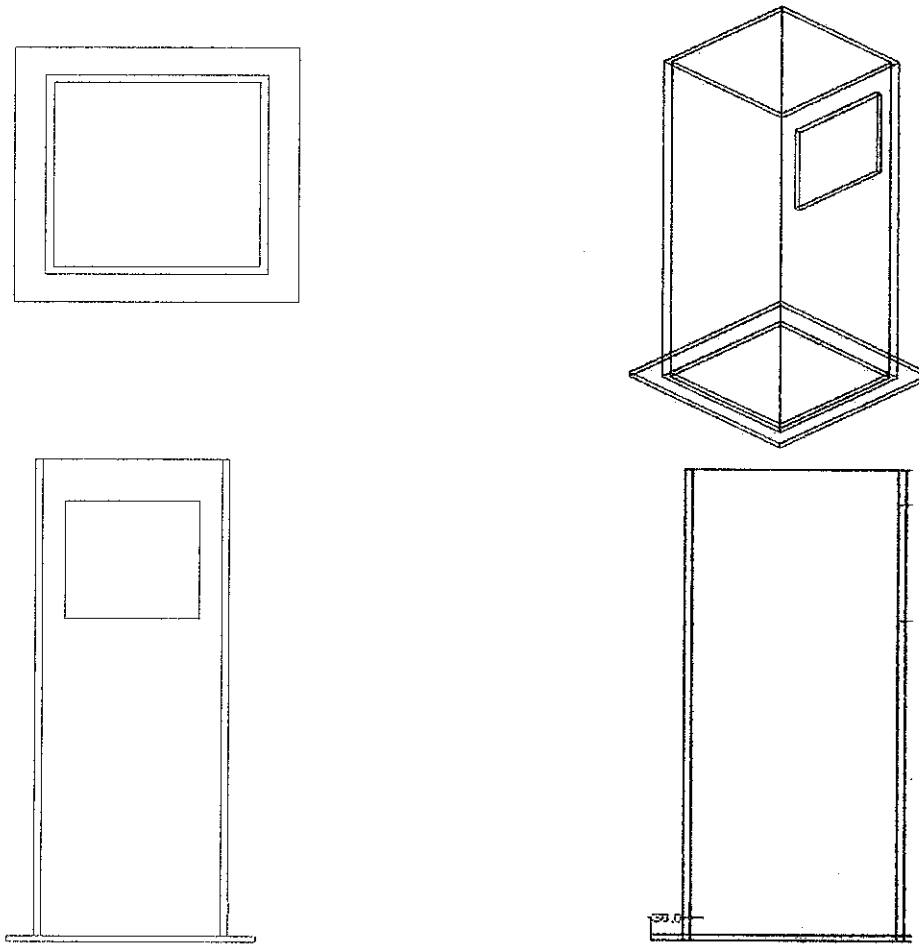


Figure 3.1: Orthographic drawing of Main Compartment.

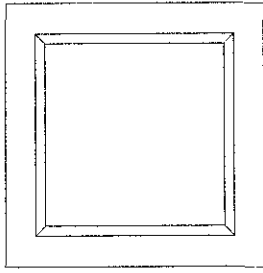


Figure 3.2: Orthographic drawing of Diffuser Compartment.

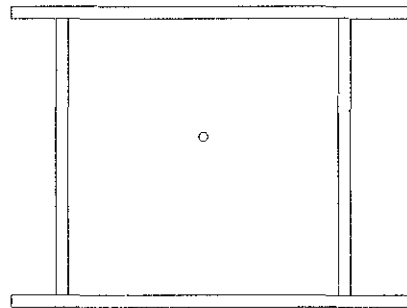
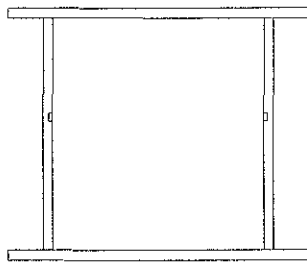
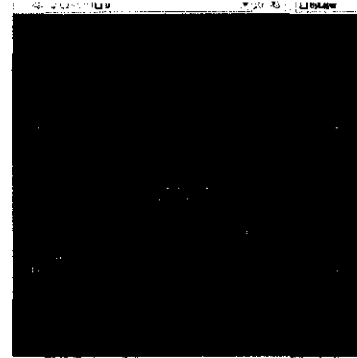
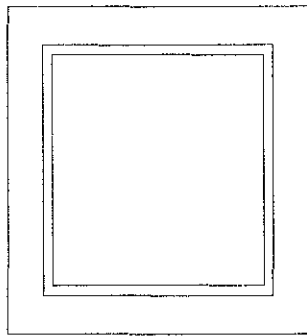


Figure 3.3: Orthographic Drawing of Damper Flapper Compartment.

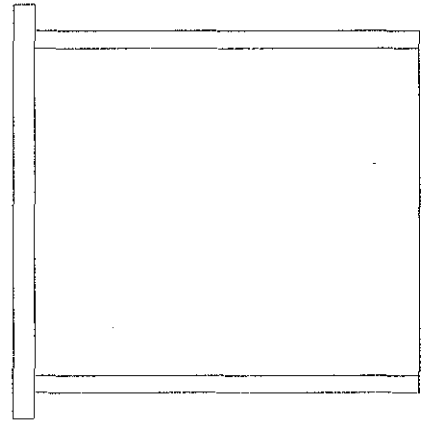
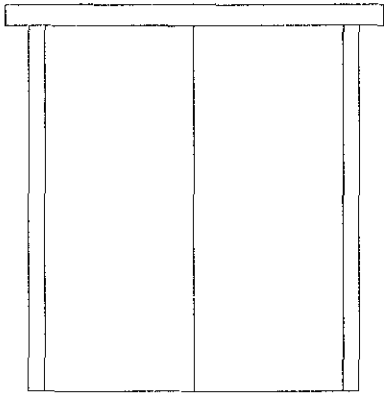
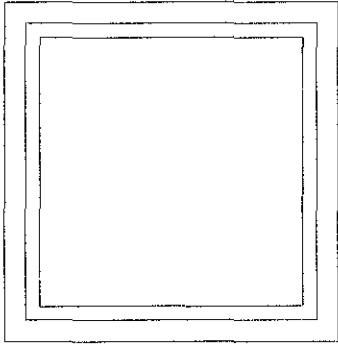


Figure 3.4: Orthographic Drawing of Outlet Nozzle.

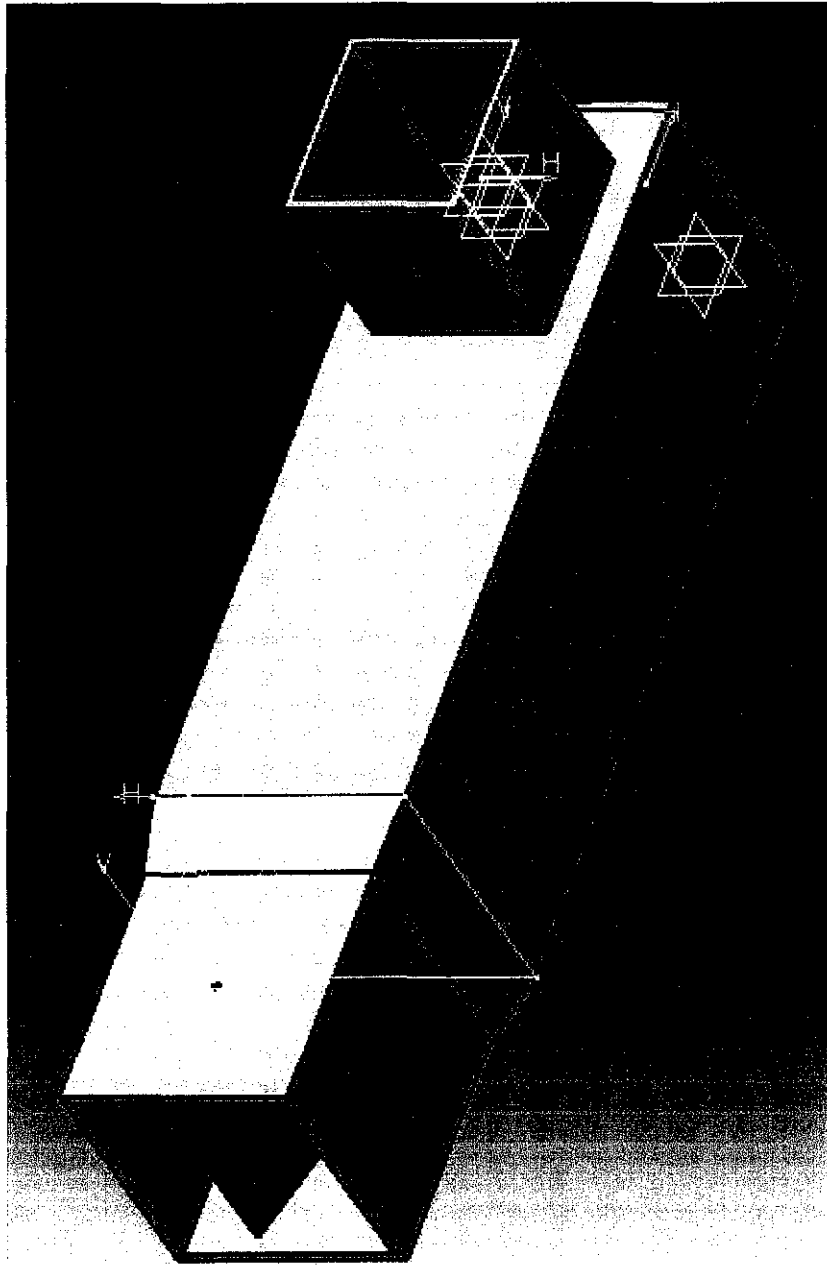


Figure 3.5: Test rig assembly.

3.4 Fabrication.

The fabrication of the main compartment, diffuser compartment, damper flapper compartment and outlet nozzle were done by the laser-cutting service provider. The gaskets and visualization kit were hand made by the author.

3.4.1 Test rig.

The main shell of the test rig was primarily made of Perspex plates, 8mm thick, attached by adhesive and sealed using silicone gel. Perspex was selected because it fulfils the condition for the shell to be transparent to enable visualization of the flow outside the test rig. To ease the placing and removing, the test rig was fabricated in compartments that attach to one another with Perspex fixtures and bolts.

Compartment 1: Main compartment.

Made up of 4 equal 600mm X 200mm Perspex plates attached to a 195mm X 195mm base plate with thickness of 8mm.

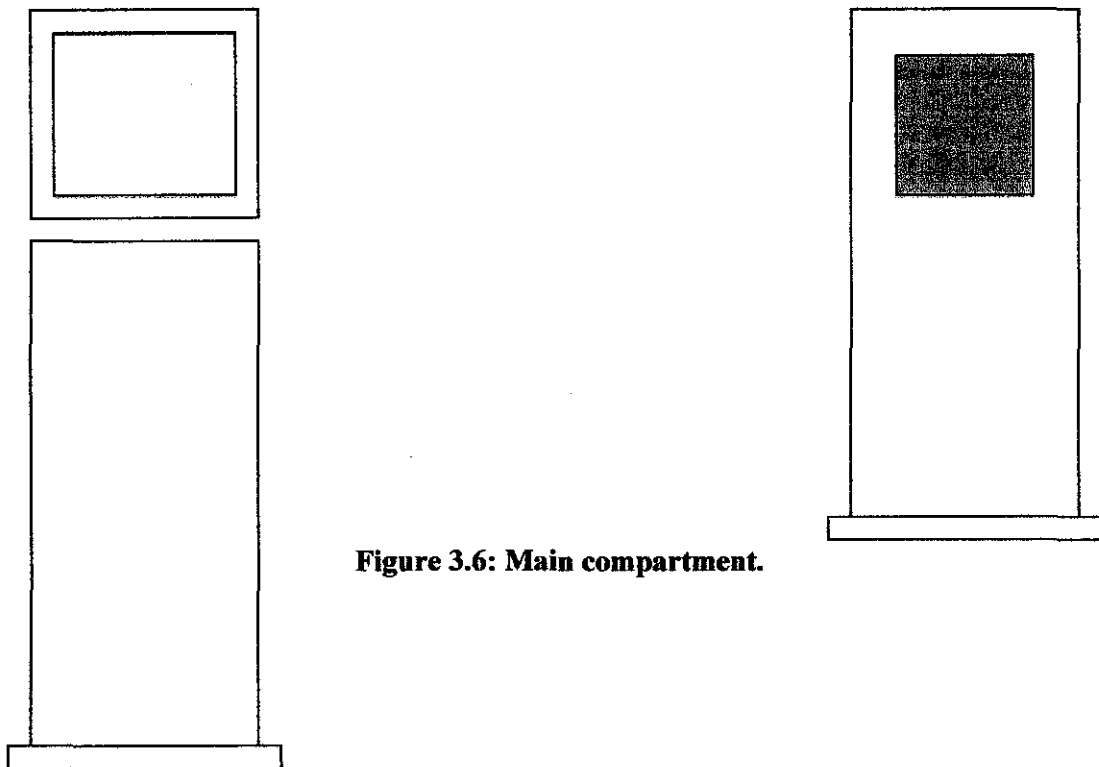


Figure 3.6: Main compartment.

Compartment 2: Diffuser compartment.

The diffuser compartment situated above the damper flapper compartment was the most delicate compartment to fabricate. The 4 sided polygons required absolute precision with angle of 11° and 79° to ensure symmetry in each of the four identical plates. All edges were carefully chamfered at an angle of 45° for each plate to attach to one another creating the diffusion or otherwise funnel-like shape. With laser cutting, the pieces were cut to precision and attached using chloroform and strengthened with 90° angled Perspex at each corner. This was the most costly section of the test rig but it was necessary given the stresses acting on this part.

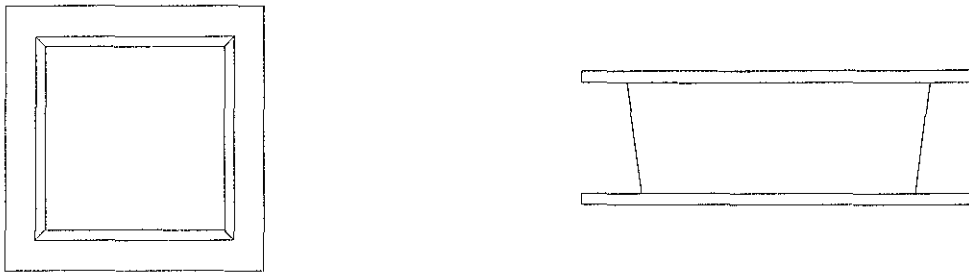


Figure 3.7: Diffuser compartment.

Compartment 3: Damper flapper compartment.

One damper flapper was housed in 180mm X 180mm X 150mm Perspex shell. The flapper made of zinc plate, 1mm thick, slotted into Perspex cylindrical shafts and secured with a rivet on either side. The shaft extended to the outside of the waterproof shell where it was attached to the main controller. To ensure there were no leaks, an O-ring was placed in an end milled slot secured in the Perspex wall.

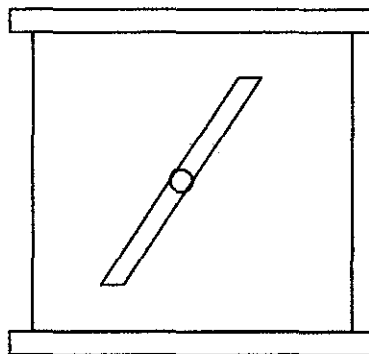


Figure 3.8: Damper flapper compartment.

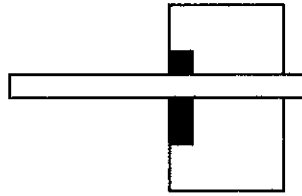


Figure 3.9: O-ring placement in the Perspex shell.

Compartment 4: Outlet nozzle.

Made up of 4 equal 150mm X 150mm Perspex plates attached to a 195mm X 0.195mm base plate with a thickness of 8mm.

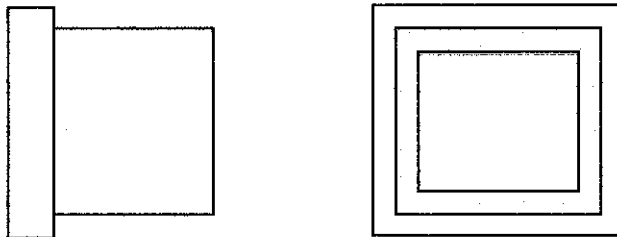


Figure 3.10: Outlet nozzle.

Compartment 5: Water container.

A plastic toolbox size 510mm X 400mm X 260mm is modified to be as a water container. An inlet hole, 1inch in size, was drilled at of the toolbox side. The top of the toolbox will be bolted with a perspex cover.



Figure 3.11: Water container.

3.4.2 Visualization kit.

For ease of viewing the flow pattern past the damper flapper, a dye injecting unit was installed below the damper flapper compartment. This unit comprised of 2 injector needles secured to a duct connected to a bottle containing the blue dye.



Figure 3.12: The visualization Kit.

3.4.3 Gaskets.

The gaskets were made up of aluminium sheet 0.5mm thick using knife and scissors. This gasket will assembled along with silicone to avoid any further leaking problem.

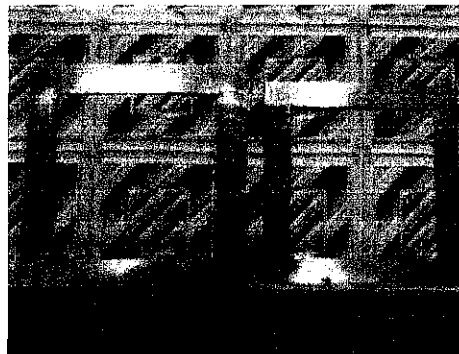


Figure 3.13: Gaskets.

3.4.4 Base of the test rig.

This base was made up from a 2ft X 4ft of plywood. Some rectangular woods were used to fabricate as a frame for the base and also as a frame for the container. The pump also bolted on this base.

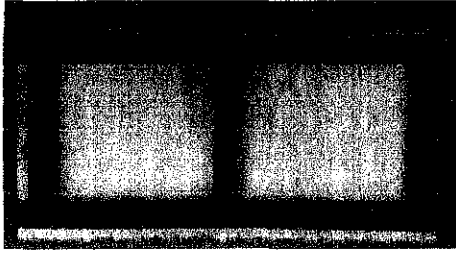


Figure 3.14: Bottom view of the

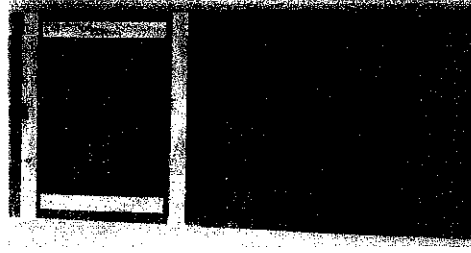


Figure 3.15: Top view of the base.

3.4.5 Top cover of the container.

This cover fabricated using 6mm X 445mm X 550mm perspex. This cover will be attached to the water container. The furnace top model will be bolted onto this cover.



Figure 3.16: Top cover of the container.

3.4.6 Piping system.

The piping system fabricated using 1 inch diameter of pvc pipes and also 1 inch of polyurethane pipes. The necessary fittings also used to connect all of these pipes. This piping system starts from the water reservoir tank into the pump and from the pump into the drainage system. From the drainage system the pipes connected to the water container via the polyurethane pipes.

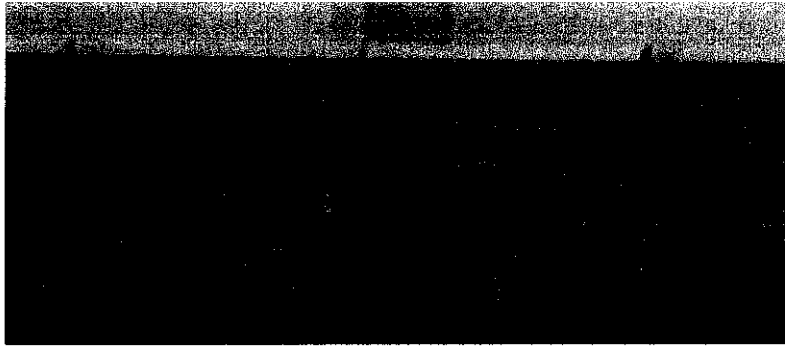


Figure 3.17: Piping system.

3.4.7 Tee support.

The tee support is fabricated to provide a resting structure for the pipe. It is fabricated using 3 pieces of rectangular wood and attached together with nails.



Figure 3.18: Tee support.

3.5 The pump requirement.

A Pump Performance Curve is produced by a pump manufacturer from actual tests performed and shows the relationship between Flow and Total Dynamic Head, the Efficiency, the NPSH required, and the BHP Required. Below is the basic factor when choosing a pump:

Higher Head = Lower Flow

Lower Head = Higher Flow

Lower Flow = Lower Horsepower

Higher Flow = Higher Horsepower

The available pump in the campus has the specification of 0.4 HP and 14m head that could only deliver a maximum flow of 80liter/min which translates to 0.0013 m³/s. the required flow rate is approximately 0.0526 m³/s (see **APPENDIX I** for calculation). With that, the flow could not occupy the entire test rig because the pump cannot deliver enough flow rates. To overcome this problem there is a need to choose the right pump. This test rig would only require high flow rate rather than the total displacement head. This is because the experiment only requires a visualization of the flow, not dealing with high head pressure. So there is a need for a better pump with better flow rate. The available pump is the centrifugal pump that can give high total displacement head, low flow rate and low horsepower. In my opinion, the axial pump is more adequate for this experiment since it has better flow rate than the centrifugal pump. The reason is, this experiment only needs the high flow rate to visualize the flow in the test rig and the total height of the test rig is only 1.5m. If we use centrifugal pump, we cannot deliver the desired flow rate. The centrifugal pump only can handle high total displacement head, for example to deliver water from ground floor of a building to the second floor. Whereas the axial flow pump is used for dealing with high capacity of flow rate such as raw water pumping application

3.6 Material procurement

The main criteria for determining the material and services required to build the test rig include; transparency for flow visualization, manageable scaled down size, strong edges and corners to sustain high pressure water, and convenient to measure pressure drops across the test section. Several compartments, particularly the square outlet nozzle, main compartment, diffuser compartment and the damper flapper compartment were specially ordered with router and laser cutting service provider while the water container was ordered with billboard service provider.

3.6.1 Inventory list

The following is the list of materials, services and consumable materials along with the size, units and cost. Some materials are left without any cost as the materials have been obtained in-house and already available in campus.

Table 3.1: Item Purchased/Obtained for Fabrication

No.	Description	Size	Quantity	Cost
				(RM)
1	Water pump	1 HP	1	250
2	Sand paper	-	1	1
3	Saw	-	1	10
4	Tubing	8mm \varnothing X 12192mm	-	20
5	Plywood	1219.2mm X 2438.4mm	1	55
6	Connector	-	7	14
7	Aluminium sheet	304.8mm X 609.6mm	1	-
8	Pipe fittings	25.4mm \varnothing	12	30
9	Pvc pipe	25.4mm \varnothing X 2743.2	1	24
10	Pipe tape	-	4	4
11	Contact adhesive	-	2	8
12	Water container	609.6 mm X 304.8mm X 304.8mm	2	100
13	Hose	25.4mm \varnothing X 609.6mm	1	15
14	Fasteners	-	50	-
15	Dye injector	-	2	-
16	Siphone tube	5mm \varnothing X 5000mm	1	9.9
17	Dye container	-	1	-
18	Water tap	25.4mm \varnothing	1	3.5
19	O-ring	-	6	3
20	Polyurethane hose	25.4mm X 3000mm	1	5
21	Damper Flapper compartment	180mm X 180mm X 150mm	1	-
22	Diffuser compartment	-	1	-
23	Main compartment	-	1	-

24	Outlet compartment	-	1	-
25	Polyurethane tee	-	1	4.8
TOTAL (RM)				557.2

Table 3.2: Consumable Purchased/Obtained for Fabrication.

No.	Description	Size	Quantity	Cost (RM)
1	Silicone	-	2	16
2	Pipe glue	-	1	3
TOTAL (RM)				18

3.7 Methodology of the experiment.

When the working fluid or water pumped into the supplementary container, the flow will become a well developed square flow. Then the water will flow into the damper flapper compartment, diffuser compartment, and main compartment. Hopefully there are enough flow rates to make sure that the working fluid will flow into the outlet compartment. The flow rate will be controlled and ranging from $0.00\text{m}^3/\text{s}$ to $0.0526\text{m}^3/\text{s}$. The damper flapper will be positioned into 20° , 40° , 60° , 80° and 90° position. The point 1 until point 5 will be connected to the manometer panel via tubing. Manometer panel will measure the pressure which is varies according to the change of the flow rate and the angle of damper flapper. The visualize flow within the furnace top with the help of the dye injector kit will be captured.

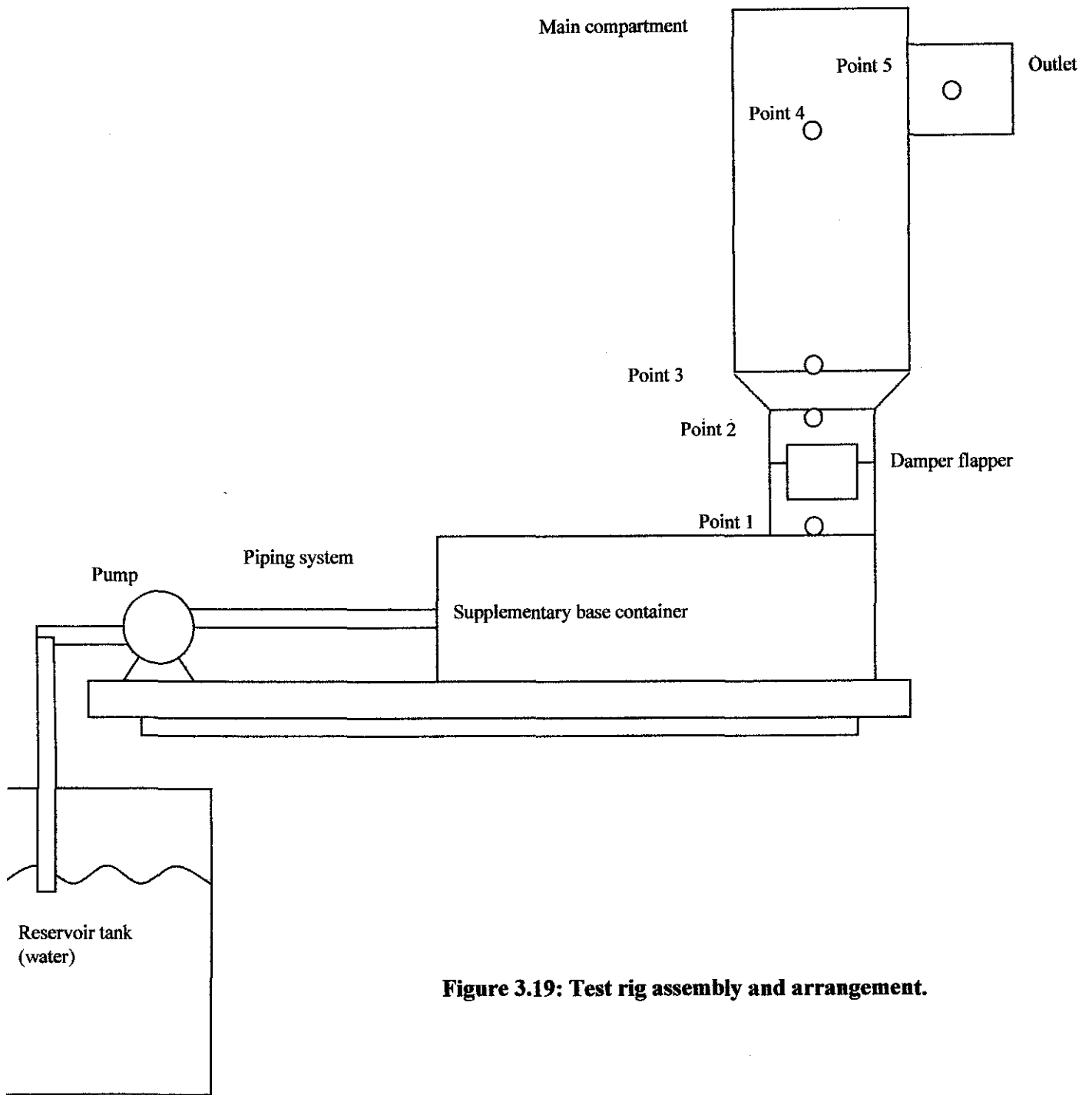


Figure 3.19: Test rig assembly and arrangement.

CHAPTER 4

RESULTS AND DISCUSSIONS

This chapter will discuss about the **RESULTS** of the experimentation. The flow visualization was successfully obtained while the pressure variation within the furnace top model was not obtained due to malfunction of the manometer. The flow was captured using video filming and is available in the attached **DVD-R**.

This chapter also discuss about the interpretation of the flow visualization hence the probable root cause will be determined.

4.1 Results.

The flow rate used in this experiment is $0.00014\text{m}^3/\text{s}$ ($\text{Re}=694.44$) and $0.000162\text{m}^3/\text{s}$ ($\text{Re}=803.57$). At each flow rate, the angles of the damper flapper were varied from 20° , 40° , 60° , 80° , 90° , and 100° to visualize the flow pattern through the injected dye. The free rotating damper flapper also visualized.

4.1.1 Flow Visualization.

Please refer to the attached **DVD-R**.



Figure 4.1: Sample Images of Flow Visualization.

4.2 Discussion.

4.2.1 Interpretation of the Results.

The leaking problem within the test rig were partially countered where there is only small leaks at the assembly of the damper flapper since it has to be rotated for the flow visualization. From the footage, just downstream of the damper flapper, there is some amount of turbulence due to the exerted fluid pressure at the top of the damper flapper compartment.

Flow rate.

When the flow rate into the test rig was increased, the amount of the induced turbulence was also great. When the flow rate increases, the flow pattern at the upstream and downstream of the flapper visualize that there is a great amount of turbulence induced at that section. However, the distance which turbulence may propagate into the test rig was unknown. This generalization shall apply to all the subsequent interpretations and will not be repeated.

Angle of damper flappers.

The damper flapper section acts like a venturi where in the flow accelerated into the contraction and decelerated as it moved downstream into the diffuser compartment.

The degree of this acceleration and deceleration was very much dependent on the angle of the damper flapper. The magnitude of the angle deflection was measured with respect to the vertical axis. The angles of the damper flapper were varied from 20°, 40°, 60°, 80°, 90°, and 100°.

As the angles of the damper flapper increases, the amount of the turbulence generate upstream and downstream of the damper flapper also increases. When the angles increases, the flow will greatly distorted by the flapper. This will generate high induced turbulence in the damper flapper compartment.

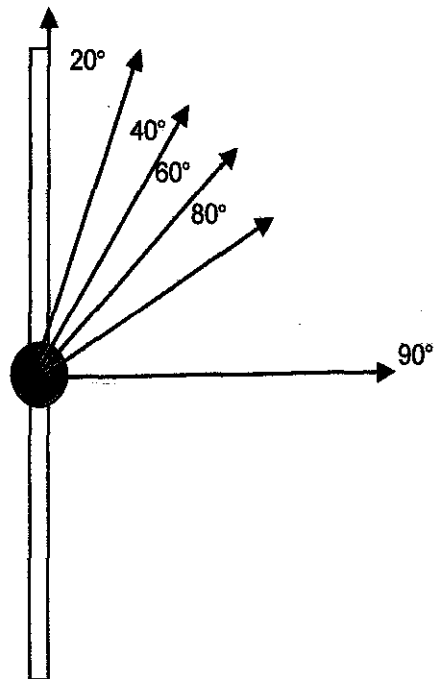


Figure 4.2: The positions of the damper flapper.

Free rotating damper flapper.

The induced turbulence was higher when the damper flapper was allowed to rotate freely. This cause a tremendous flow distortion in the form of eddies and swirls.

4.2.2 Probable root causes.

Flow rate.



Figure 4.3: 20° angle of damper flapper position with flow rate of 0.00014m³/s (Re=694.44) on the left and 0.000162m³/s (Re=803.57) on the right.

The increasing flow rate into the test rig will greatly induced the turbulence. From the footage above, we can see when the flow hit the damper flapper; turbulence will induce at that section. This scenario will create higher turbulence intensity with increasing flow rate.

Angles of damper flapper.



Figure 4.4: Damper flapper with increasing angles.

From the footage above, clearly we can see that at the section of the upstream and downstream of the damper flapper, there will be increase in turbulence intensity when the angle increases. Thus the angle of the damper flapper also effect the generation of the induced turbulence.

Free rotating damper flapper.

Once the flapper was inclined to one side, the dynamic pressure below the inclination was lower than the top. This will result in the static pressure to increase at the bottom and decrease at the top, causing the flapper to rotate and inline in the opposite direction. This process repeated itself for as long as the given conditions inside the furnace maintained. The free rotating damper flapper induced swirls and eddies, that propagated downstream, causing vibration and noise and hence, the inductor fan lodging itself into the cowling.

4.2.3 Compressibility of the fluids.

When the fluid achieves a Mach number greater than 0.3, then the fluid is incompressible [6]. From the calculations (Refer to **APPENDIX I**), the flue gas is incompressible at a velocity of 8.315 m/s thus there is no time dependant varying density gradient in the flow duct. For water, the Mach numbers indicate that the flow is incompressible thus the continuity equation can be applied.

4.2.4 Limitations.

Inviscid flow assumption.

Any fluid flow passing an immersed body will generate friction. This friction induced by the wall shear stress. The region where experiences the effect of the shear stress is known as the boundary layer. For ease of the calculating driver and pump requirements for the test rig, the fluid was assumed to be inviscid, as Perspex has a very low surface roughness which is almost zero. It allows some value of deviation from the actual results.

Steady state assumption.

The steady state assumes no time rate of change of the velocity and hence, the momentum of the fluid in question within the control volume, which is the furnace top or the test rig. However this is not possible. The fluid will experience contractions and expansion when flow through diffusers, nozzles and bends. It will cause the fluid to alternately decelerate and accelerate instantly several times, resulting in a change in velocity and hence momentum.

Composition of flue gas.

The properties of the flue gas was obtained from APPENDIX I to generate the Reynolds number since the flue gas composition of the actual furnace in EPMSB, Paka was unavailable. It is assumed that the cracking process of ethane uses the refined ethane that contains no sulphur, completely combust to produce only nitrogen, carbon dioxide and water molecules. Ideally the composition of the flue gas should include fluids such as ethane, carbon dioxide, carbon monoxide, water, oxygen and nitrogen.

Dimensionless parameters.

The Reynolds number provides the similarity between the inertial and viscous forces. The actual flue gas temperature was 200°C but in this analysis, the fluid used to model the flow is water at room temperature. When using different fluid with different properties such as density and dynamic viscosity value to generate a model of prototype using air as working fluid, there are limitations in meeting all the dimensionless parameter.

The typical Prandtl number of gases is approximately 0.7 [7] while for liquids the value range approximately to 7. Liquids exhibit lower dynamic viscosity when heat is added because of the intermolecular bonds has ample energy to break and thus, release vapor. For gases, the molecules are parts away from each other with negligible

intermolecular forces. Heat addition will provide more energy to the molecules to collide with each other and the wall in which they are contained in, making the fluid more viscous. The higher Prandtl number means that the heat diffusion via convection is dominant, unlike for gas, as a result of the characteristics of liquids and gas mentioned above. Thus, this dimensionless parameter cannot be matched.

The Nusselt number, Nu , is the ratio of heat transfer via convection through the surfaces in which the fluid is contained to that of the heat transfer via conduction alone, through the same surface. The Nusselt number also cannot be matched because, the temperature of the flue gas flowing at the mainstream and surface of the duct is not available. Even with that information, both the working fluid and the walls of the model are not at the same temperature and there is negligible heat transfer. Then the Nu became zero for the model.

Therefore the test rig is limited in its capability in similarity between the fluid flows in the actual furnace top. The experiment expected only to calculate the effect of velocity differences, translating into the rate of change of momentum, hence the force the fluid exerts along the path in which the velocity differences are experienced. The force exerted on the furnace top as a result of heat conduction and convection between the fluids and the conduit surface and the surrounding, is left as speculation.

Pump capacity.

The pump used for the experimentation was not adequate for the experiment. There was no axial pump available in the campus, which is the best pump type to conduct the experiment. Thus, a centrifugal pump with a capacity of 1HP was used where it also cannot deliver the desired flow rate.

Air pockets.

The working fluid, water, pumped into the water container and flow into the test rig. However, there are air pockets trapped in the water container. Additional pressure of the working fluid will only cause the air pockets to compress but never escape. There

is a need to install a bleed valve at the water container to bleed out the air trapped in the water container.

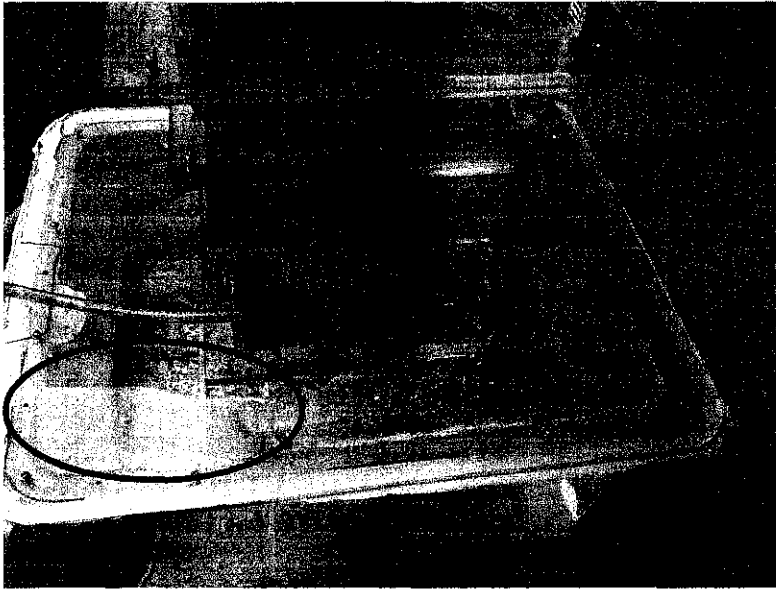


Figure 4.5: The location of the air pockets.

CHAPTER 5

CONCLUSION AND RECOMMENDATION

5.1 Conclusion.

As a conclusion, to guarantee the successful of this experiment, there is a need to use an axial flow pump. The reason is since the axial flow pump can give a better capacity or flow rate rather than using a centrifugal pump. The required flow rate is $0.0526 \text{ m}^3/\text{s}$. With the axial flow pump, high flow rate pump, the other problem during the experiment such as leaking will be no big deal. For the leaking problem, that problem is successfully encountered using the silicone gasket.

Some assumptions had to be made to conduct technical calculation and to design the model. These assumptions caused some amount of deviation from the actual results, however within limits, to fulfil the objectives of the Final Year Project.

The dimensionless parameter matched (Re) allowed an analysis of the effects of velocity differences on the force exerted on the test rig components. The dimensionless parameter for heat diffusion and heat transfer could not be matched thus the force exerted to the test rig due to such heat dynamic was not considered in the analysis.

Modelling and Simulation of Furnace Top in 3-D.

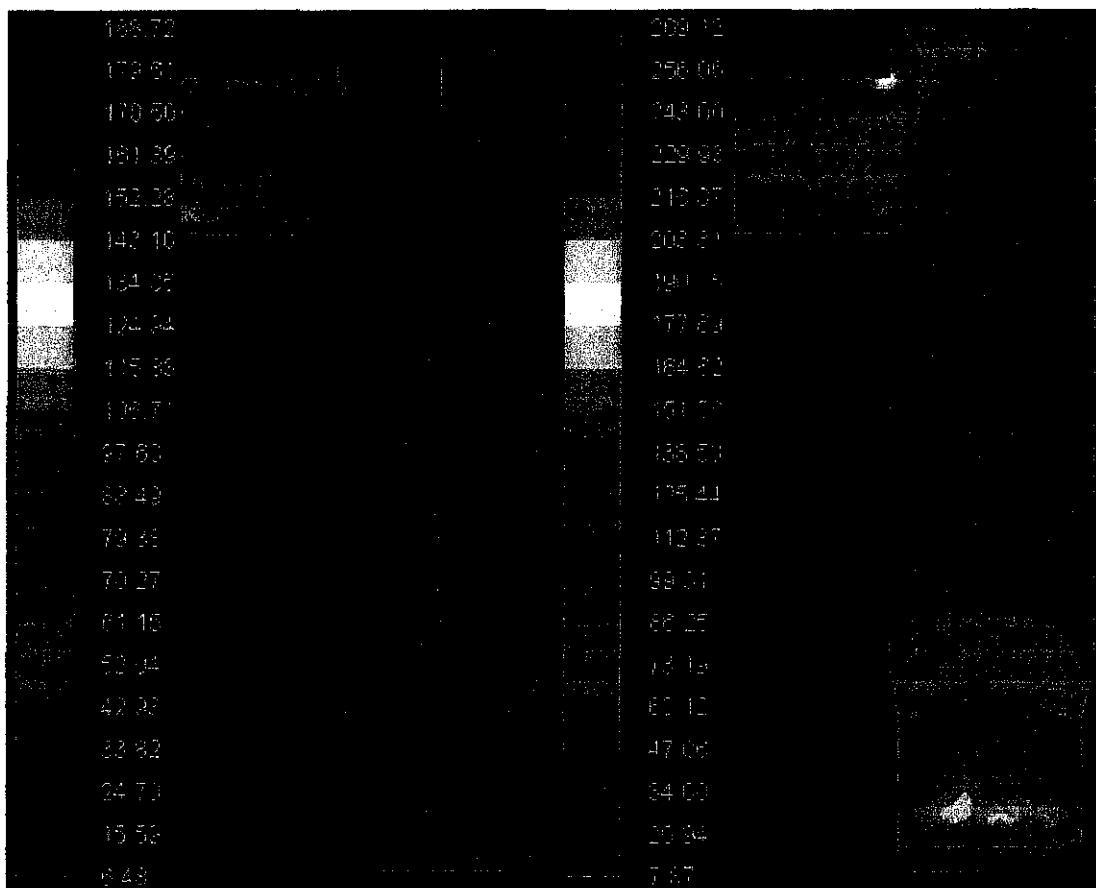


Figure 5.1: Comparison of Turbulence Intensities (%) Before (Left) and After (Right) Damper Flapper Failure for 0° (Vertical) Angled Damper Flappers. [16]

In Figure 5.1 above, the turbulence intensities are shown for when the damper flappers are in a 0° angles before and after failure. This view from the right shows clearly the turbulence at the outlet points of the furnace top, which also are the areas where the cowling and furnace fan are located. As can be seen, in the simulation with the failed damper flapper system, there is a clear increase in turbulence intensity at the outlet area. The highest increase in the turbulence intensity can be seen at the top part of this outlet (colour yellow). The highest turbulence intensity in the failed damper flapper system is 190% whereas in the fully functional damper flapper system, turbulence intensities only reach 100% around the outlet area. [16]

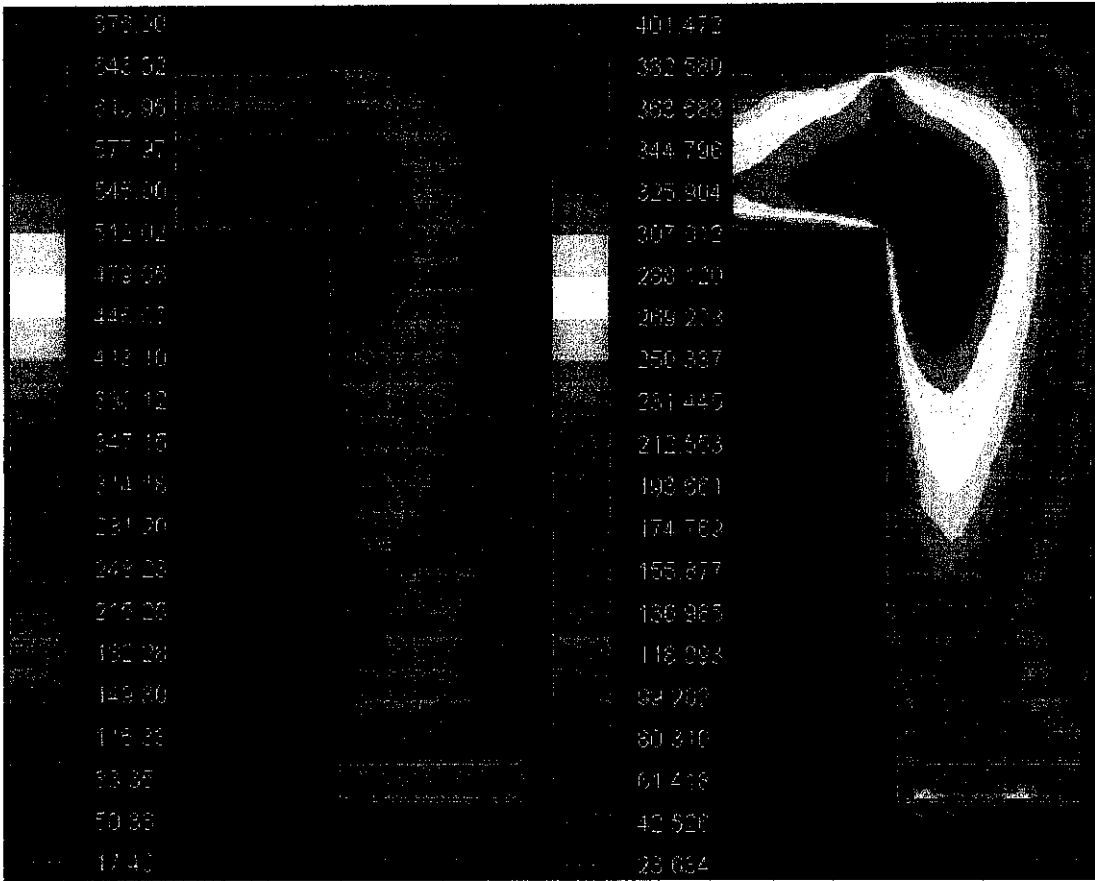


Figure 5.2: Comparison of Turbulence Intensities (%) Before (Left) and After (Right) Damper Flapper Failure for 45° Angled Damper Flappers. [16]

Again in the Figure 5.2 above, a similar trend could be seen as that in Figure 5.0. The turbulence intensities reached 400% in the failed damper flapper system, but only managed to reach 350% in the fully functional system. This clearly shows that the failure of the damper flapper system did cause an increase in turbulence intensities at the outlet area where the cowling and furnace fan are located. [16]

The simulation shows higher turbulence after the damper flapper system failed. These can be observed more clearly at certain areas of the furnace top at certain damper flapper angles. The most obvious increases in turbulences can be seen in the 0° and 45° angled damper flappers and the area which shows the most increase are the walls of the furnace top and the outlet area. These higher turbulence intensities could have aggravated and contributed to the wear and tear on the cowling causing it to fail. Therefore the failure of the damper flapper system, did contribute to an increase in turbulent flow which in turn could have caused the failure of the fan furnace.

Flow visualization indicated that the rotational motion of the loose damper flapper resulted in induced turbulence, distorting the typical flow patterns. This induced turbulence was greater when:

- 1) **Increased flow rate** into the test section.
- 2) The **divergences of the angles of damper flappers** with respect to the vertical axis.
- 3) The loose damper flapper **rotated at a higher frequency**.

The objectives of this Final Year Project were partially met as there were malfunctions in the equipment which were beyond the control of the candidate. Nevertheless, the author was able to postulate two root causes of the induced turbulence that are:

- 1) The angles of the damper flapper.
- 2) The damper flapper left to rotate causing induced turbulence downstream.

The pressure measurement within the test rig cannot be recorded due to the malfunction of the manometer. Manometer panel will measure the pressure which is varies according to the change of the flow rate and the angle of damper flapper. The pressure variation and fluctuations within the test rig will confirmed the failure of the damper flapper contributed the generation of high induced turbulence which have could cause the failure of the induction fan. So the pressure fluctuations within the test rig when the damper flapper fails (free rotating damper flapper) was not determined.

The best practice to prevent this incident is to practice very effective preventive maintenance. Honeycomb and screen can be incorporated into the design of the furnace top to reduce the amount of induced turbulence. Honeycombs are generally used as flow directionalizers-stabilizers and/or to reduce lateral components of turbulence in a flow. A honeycomb naturally produces some turbulence of its own. With eddy sizes of the same order as the cell diameter, which decays very much

slowly than that of which created by screens. The honeycomb is best placed just upstream of the test section to streamline the flow.

5.2 Recommendation.

It is recommended for UTP to purchase a better pump such as an axial flow pump. This type of pump can operate in wide range of pressures, have higher discharge pressures than centrifugal pumps for less power consumption, has better suction lift than centrifugal pumps, 20% more efficient than centrifugal pumps, and also has accurate volume control. The current design of the furnace top could be improved to reduce the risk of failure. Simulation should be done to determine the optimum design in which the risks of failure are minimal.

The preventive maintenance would be the best resolution to prevent this incident altogether avoiding lost production hours and unmet targets that was crucial. Proper maintenance procedures for replacement of the cotter pin and the damper flapper system as a whole should be drafted and adhered to strictly to avoid such reoccurrence. Proper personnel training also need to be carried out to practice the preventive maintenance.

It is also recommend that a honeycomb must be placed just upstream of the damper flapper section to streamline the flow into the section [11]. However, the honeycomb also recommended being installing just downstream of the damper flapper section in case of the induced turbulence due to loose or failed flapper. This honeycomb use to streamline the induced turbulence propagated out of this section. Further experimentation should be carried out on the design of the honeycomb.

Further enhancement of the test rig and experiment.

More information pertaining to the properties of the fluid, weight and material of the damper flapper, lever arm and cotter pin. For the damper flappers, it would help to determine the position or alternatively the motion in which the damper flapper was during the incident.

- 1) Damper flappers are controlled using gears to enable a full span of rotation from completely open to completely close.
- 2) Need to use the axial flow pump to deliver the required flow rate for the test rig since it can deliver much higher flow rate rather than using centrifugal pump.
- 3) Use an inductor fan in place of a pump to create the rotational flow effect.
- 4) A bleed valve fitted at the water container as well as the top of the test rig to bleed out the air pocket and enable working fluid to assume the volume of the entire test rig.
- 5) Since the pressure variation could not be recorded due to the manometer malfunction, it is recommended to use the pressure gauges for each point within the test rig, connected via tubing.

REFERENCE

- 1) ASHRAE (1992). ASHRAE Handbook. Heating, ventilating and air-conditioning systems and equipment.
- 2) The Properties of Petroleum Fluids; Second Edition; William D. McCain, Jr.
- 3) Emerson Process Management Rosemount Analytical Inc. Process Analytic Division.
- 4) A Brief Introduction to Fluids Mechanics 3rd Edition, Young, Munson and Okiishi.
- 5) <http://www.answers.com/topic/transitional-flow?cat=technology>.
- 6) "Experimental Modelling Of The Fluid Flow In A Furnace Top Of An Ethane Cracker In EPMSB, Paka" by Thanavathy A/P Patma Nesan.
- 7) <http://www.gouldspumpsashland.com/Axial-Flow-Pump.htm>.
- 8) <http://www.carrymfg.com/axial.htm>.
- 9) <http://www.gouldspumpsashland.com/Centrifugal-Pump.htm>.
- 10) <http://pump-zone.com/article.php?articleid=337>.
- 11) Tom Bitzer 2007, Honeycomb Technology: Materials, Design, Manufacturing, Application and Testing, 3rd Edition, Chapman and Hall.
- 12) Maintenance Instructions Mars® 100 Gas Turbine-Driven Mechanical Drive Set, Petronas West Natuna (Duyong), DR REF: 2HG-4PK.
- 13) <http://www.efunda.com/formulae/fluids/manometer.cfm>.
- 14) <http://www.upscale.utoronto.ca/PVB/Harrison/Manometer/Manometer.html>. (Written by David M. Harrison, Dept. of Physics, Univ. of Toronto, harrison@physics.utoronto.ca, in July 2002. All text and images are Copyright © 2002 David M. Harrison.)
- 15) <http://www.patentstorm.us/patents/5463159-claims.html>.
- 16) Simulation of the Flow in the Furnace Top of an Ethane Cracker at EPMSB Paka by Tomi Tulin Entaban Anak Watt Lanyau.

- 17) <http://en.wikipedia.org/wiki/Furnace>.
- 18) http://en.wikipedia.org/wiki/Laminar_flow.
- 19) http://en.wikipedia.org/wiki/Axial_flow_pump.
- 20) <http://en.wikipedia.org/wiki/Honeycombs>.
- 21) http://en.wikipedia.org/wiki/Flue_gas_stack.

APPENDIX I

Reynolds Number calculation.

Volumetric flow rate, $Q = 15.4 \text{ m}^3 / \text{s}$

Kinematics viscosity, $\nu_{flue} = 3.28 \times 10^{-5} \text{ m}^2 / \text{s}$ flue gas at 200°C

Inlet:

$$\text{Inlet Area, } A_{inlet} = 1.8 \text{ m} \times 1.8 \text{ m} = 3.24 \text{ m}^2$$

$$\text{Inlet Perimeter, } P_{inlet} = 1.8 + 1.8 + 1.8 + 1.8 = 7.2 \text{ m}$$

Inlet Equivalent Hydraulic

$$\text{Diameter, } D_{inlet} = 4A / P = 12.96 \text{ m}^2 / 7.2 \text{ m} = 1.8 \text{ m}$$

$$Q_{inlet} = V_{inlet} \times A_{inlet}$$

$$V_{inlet} = \frac{Q_{inlet}}{A_{inlet}} = \frac{15.4}{3.24} = 4.753 \text{ m} / \text{s}$$

$$\text{Reynolds Number, } Re = \frac{V_{inlet} \times D_{inlet}}{\nu_{flue}} = \frac{4.753 \times 1.8}{3.28 \times 10^{-5}} = 260835$$

Outlet:

$$\text{Outlet Diameter, } D_{outlet} = 1.5 \text{ m}$$

$$\text{Outlet Area, } A_{outlet} = \pi \frac{D_{outlet}^2}{4} = \pi \frac{1.5^2}{4} = 1.767 \text{ m}^2$$

$$Q_{outlet} = V_{outlet} \times A_{outlet}$$

$$V_{outlet} = \frac{Q_{outlet}}{A_{outlet}} = \frac{15.4}{1.767} = 8.715 \text{ m} / \text{s}$$

$$\text{Reynolds Number, } Re = \frac{V_{outlet} \times D_{outlet}}{\nu_{flue}} = \frac{8.715 \times 1.5}{3.28 \times 10^{-5}} = 398534$$

Calculation for velocity model.

With 1:10 scale model prototype and water as working fluid.

Kinematics viscosity, $\nu_{water} = 1.12 \times 10^{-6} \text{ m}^2 / \text{s}$ water at 15.6°C .

$$\text{InletArea, } A_{inlet} = 0.18m \times 0.18m = 0.0324m^2$$

$$\text{InletPerimeter, } P_{inlet} = 0.18 + 0.18 + 0.18 + 0.18 = 0.72m$$

Inlet Equivalent Hydraulic

$$\text{Diameter, } D_{inlet} = 4A / P = 4 \times 0.0324m^2 / 0.72m = 0.18m$$

$$\text{Reynolds Number, } Re = 260835$$

To achieve the same Reynolds Number:

$$\text{ReynoldsNumber, } Re = \frac{V_{inlet} \times D_{inlet}}{v_{flue}} = \frac{V_{inlet} \times 0.18}{1.12 \times 10^{-6} m^2 / s}$$

$$\text{ModelInletVelocity, } V_{inlet} = \frac{Re \times v_{water}}{0.18} = \frac{260835 \times 1.12 \times 10^{-6} m^2}{0.18} = 1.623m / s$$

Outlet:

$$\text{OutletDiameter, } D_{outlet} = 1.5m$$

$$\text{OutletArea, } A_{outlet} = \pi \frac{D_{outlet}^2}{4} = \pi \frac{0.15^2}{4} = 0.01767m^2$$

$$\text{Reynolds Number, } Re = 398534$$

To achieve the same Reynolds Number:

$$\text{ReynoldsNumber, } Re = \frac{V_{outlet} \times D_{outlet}}{v_{flue}} = \frac{V_{outlet} \times 1.5}{1.12 \times 10^{-6} m^2 / s}$$

$$\text{ModelOutletVelocity, } V_{outlet} = \frac{Re \times v_{water}}{0.15} = \frac{398534 \times 1.12 \times 10^{-6} m^2}{0.15} = 2.976m / s$$

Flow rate required

$$Q = AXV$$

$$Q = 0.18^2 \times 1.623$$

$$Q = 0.0526m^3 / s$$

Driver and Pump Requirements.

Model Outlet Diameter, $D_{outlet} = 0.15 m$

$$\text{Model Outlet Area, } V_{\text{outlet}} = \frac{\pi(0.15\text{m})^2}{4}$$

$$= 0.01767 \text{ m}^2$$

$$\text{Flow rate required} = A \times V$$

$$= 0.0526 \text{ m}^3/\text{s}$$

$$\frac{V_1^2}{2g} + \frac{P_1}{\gamma} + H_p = \frac{V_2^2}{2g} + \frac{P_2}{\gamma} + H_f + Z_2$$

Z_1 = height of the test rig from ground level.

Z_2 = total elevation from ground level.

V_1 = inlet velocity = 1.623 m/s .

V_2 = outlet velocity = 3500 m/s .

g = gravity.

P_1 = inlet pressure.

P_2 = outlet pressure.

H_f = frictional losses.

h_M = major losses ≈ 0 (Perspex; negligible surface roughness).

h_L = minor losses.

H_p = head added by pump.

$$Z_1 - Z_2 = 1 \text{ m} - 0 \text{ m} = 1 \text{ m.}$$

$$\frac{V_2^2 - V_1^2}{2g} = \frac{(3500 \text{ m/s})^2 - (1.623 \text{ m/s})^2}{2 \times 9.81} = 0.4901 \text{ m}$$

$$P_1 - P_2 = 0$$

$K_L = 1$ (sharp edge diffusing section).

= 0.8 (sharp edge nozzle at outlet).

= 0.3 (flanged sharp bend before outlet).

$$h_L = \frac{K_L V^2}{2g} = \frac{[(1.0 \times 1.623^2) + (0.8 \times 3.5^2) + (0.3 \times 1.315^2)]}{2(9.81)} = 0.6602m$$

$$H_f = \sum h_m + \sum h_L = 0m + 0.6602m = 0.6602$$

$$H_p = 1m + 0.4901m + 0m + 0.6602m = 2.1503m \text{ (to overcome losses)}$$

$$\begin{aligned} \text{Discharge driver pressure to overcome losses} &= (2.1503 \times 999 \times 9.81) N/m^2 \\ &= 21073.5 N/m^2 \\ &= 21073.5 \times 10^{-5} \\ &\approx 0.22 \text{ bar} \end{aligned}$$

Compressibility of fluid in furnace top.

$$\text{Mach Number, } Ma = \frac{V}{a}$$

$$\text{Speed of sound in air, } a = (\gamma RT)^{1/2}$$

$$\text{Gas constant, } R = 286 \text{ m}^2/\text{s}^2 \cdot \text{K}$$

T = absolute temperature

$$\text{Ratio of specific heats, } \gamma = \frac{C_p}{C_v}$$

C_p = specific heat (constant pressure)

C_v = specific heat (constant volume)

$$C_p \text{ at } 200^\circ \text{C} = 1.097 \text{ kJ/kg.K}$$

Assumption: the molecular weight of Nitrogen gas is used as it constitutes 76% of the flue gas composition.

$$1.097 \text{ kJ/kg.K} \times 28 \text{ kg/kmol} = 30.716 \text{ J/mol.K}$$

$$R = 8.314 \text{ J/mol.K}$$

$$C_v = C_p - R$$

$$C_v = 30.716 - 8.314$$

$$C_v = 22.4015 \text{ J/mol.K}$$

$$\gamma = \frac{C_p}{C_v} = \frac{30.716}{22.402} = 1.371$$

$$a = (\gamma RT)^{1/2}$$

$$R = 286 \text{ m}^2/\text{s}^2 \cdot \text{K} \quad T = (200 + 273.15)^\circ\text{K}$$

$$a = (1.371 \times 286 \times 473.15)^{1/2} = 430.726 \text{ m/s}$$

$$Ma = \frac{V}{a}$$

$$Ma_{\text{inlet}} = \frac{3.85}{430.726} = 0.0089$$

$$Ma_{\text{outlet}} = \frac{8.715}{430.726} = 0.0202$$

APPENDIX II

Reynolds Number calculation.

For flow rate $Q=0.00014\text{m}^3/\text{s}$

$$v = \frac{Q}{A} = \frac{0.00014}{0.0324} = 4.321 \times 10^{-3}$$

$$\text{Re} = \frac{VxD}{\nu} = \frac{(4.321 \times 10^{-3})(0.18)}{1.12 \times 10^{-6}} = 694.44$$

For flow rate $Q=0.000162\text{m}^3/\text{s}$

$$v = \frac{Q}{A} = \frac{0.000162}{0.0324} = 5 \times 10^{-3}$$

$$\text{Re} = \frac{VxD}{\nu} = \frac{(5 \times 10^{-3})(0.18)}{1.12 \times 10^{-6}} = 803.57$$

APPENDIX III

Physical Properties of Flue Gases.

Vero International
*Computer Aided Design (CAD) and
 Computer Aided Manufacturing (CAM) software*

Physical properties of flue gases

Available tables: [dry air](#) [gases](#) [flue gases](#) [water](#) [steam](#)

This table is for flue gases. It gives values of some physical properties in relation to the temperature of gases.
 It is for following chemical composition:

- carbon dioxide CO₂ - 13%
- water vapour H₂O - 11%
- nitrogen N₂ - 76%

t	rho	c _p	mi*10 ⁵	ni*10 ⁵
[°C]	[kg/m ³]	[kJ/kgK]	[Pas]	[m ² /s]
0	1.295	1.042	15.8	12.2
100	0.95	1.068	20.4	21.54
200	0.748	1.097	24.5	32.8
300	0.617	1.122	28.2	45.81
400	0.525	1.151	31.7	60.38
500	0.457	1.185	34.8	76.3
600	0.405	1.214	37.9	93.61
700	0.363	1.239	40.7	112.1
800	0.33	1.264	43.4	131.8
900	0.301	1.29	45.9	152.5
1000	0.275	1.306	48.4	174.3
1100	0.257	1.323	50.7	197.1
1200	0.24	1.34	53	221

where is for flue gas:

- t - temperature
- rho - density
- c_p - specific heat
- mi - dynamic viscosity
- ni - kinematic viscosity